



Elemental profiling of agricultural soil in Hoshiarpur utilizing analytical techniques

Vaishali Dadwal · Deep Shikha · Sonika Gupta ·
Vimal Mehta · Raghunath Acharya

Received: 20 January 2024 / Accepted: 5 July 2024 / Published online: 30 July 2024
© The Author(s), under exclusive licence to Springer Nature B.V. 2024

Abstract Our study aimed to assess the soil quality in Punjab's Hoshiarpur district through a meticulous analysis of nutrient and elemental composition. Using a variety of analytical techniques, including Neutron Activation Analysis (NAA), external Particle-induced Gamma-ray Emission (PIGE) an Ion beam analysis Technique, and energy-dispersive X-ray fluorescence (ED-XRF), we delved into soil characterization for 22 agricultural soil samples in the Punjab region. Within the NAA framework, utilizing the Pneumatic Carrier Facility and the self-serve facility at Dhruva reactor in Mumbai, a brief 1-min irradiation procedure identified pivotal elements—Na, Mg, V, Al, Mn, and K.

Conversely, an extended neutron irradiation process of approximately 4 h within the self-serve facility enabled the estimation of nearly 12 elements, including Rare Earth Elements (REEs), Transition elements, and other significant elements. The external PIGE technique quantified low Z elements (Na, Mg, Al, and Si), contributing to our analytical arsenal. Rigorously validating both NAA and PIGE methodologies, we compared results meticulously against established geological standard reference materials—specifically USGS RGM-1 and USGS AGV-1. Instrumental in elemental analysis, ED-XRF spectroscopy fortified our investigative endeavors by quick assessment of ten crucial elements. The elemental analysis revealed notable accumulations of Mn and Zn in the soil, surpassing the suggested permissible limits, whereas Co, Cr, and Pb were found to be within the recommended thresholds set by WHO/UNEP. Beyond elemental profiling, our study extended to estimate the accumulation levels of various elements utilizing ecological risk factors such as Contamination Factor, Potential Ecological Risk Index, Pollution Load Index, and Geoaccumulation Factor. Our findings highlighted significant accumulation of REEs including La, Sm and Yb.. This evaluation sheds new light on the interplay between soil composition and environmental health, emphasizing the need for advanced accessible agricultural technologies to prevent and forecast contaminant discharge in arable soil. This commitment aligns with our broader goal of advancing sustainable practices in soil management.

V. Dadwal · D. Shikha (✉) · V. Mehta
Department of Physics, Sri Guru Teg Bahadur Khalsa
College, Sri Anandpur Sahib 140118, India
e-mail: deep_shikha79@yahoo.co.in

V. Dadwal
Department of Physics, Punjabi University,
Patiala 147002, India

S. Gupta
Radiochemistry Division, Bhabha Atomic Research
Centre, Mumbai 400085, India

R. Acharya
Isotope and Radiation Application Division, Bhabha
Atomic Research Centre, Mumbai 400085, India

R. Acharya
Department of Atomic Energy, Homi Bhabha National
Institute, Mumbai 400094, India

Keywords Arable soils · Ecological risk factors · Hoshiarpur district · Soil quality · Spectral techniques · Rare earth elements · Elemental analysis

Introduction

Comprehending soil quality involves exploring its diverse functions in the natural environment. Soil is responsible for recycling nutrients, managing rainwater flow, and providing ecosystem stability (Vasu et al., 2020). Soil holds different definitions depending on the field, such as scientists who study its physical, chemical, and biological traits that impact its quality (Lehmann et al., 2020). Their focus is on examining the interplay of these factors in soil health. Recently, soil degradation has emerged as a critical concern, particularly in arable land, attributed to imbalances in the soil's essential macro and microelements. This imbalance, subsequently reflects in crops, and may contribute to various health hazards. Over 95% of food supplements are derived from the soil, so attention to this issue becomes imperative. Soil nutrient assessment is necessary to promote sustainable and economically viable agricultural practices (Gruhn et al., 2000; Solangi et al., 2023). The current global population of 7.6 billion is projected to surge to 9.3 billion by 2050 (Dey et al., 2023, Alexandratos and Bruinsma, 2012). As this population growth continues, there will be heightened demands on land and water resources worldwide (Pimentel et al., 2004). This poses significant challenges for numerous countries like India striving to attain sustainable food security, primarily due to limited per capita land availability, scarcity of freshwater resources, and impacts of climate change. Moreover, these challenges are intensified by significant degradation of soil quality (Rosegrant et al., 2009). In India, Punjab is celebrated as one of India's leading states in agricultural production. During the Green Revolution, Punjab has unfortunately witnessed indiscriminate use of pesticides and fertilizers in its soil over the years (Kesavan and Swaminathan, 2008; Swaminathan, 2017). Previous research conducted in the Hoshiarpur region of Punjab, India (known for its seleniferous land) revealed that agricultural land was impacted by elevated levels of selenium (Se), which was taken up by various crop plants including wheat, maize, rice, and their by-products, thus entering the

human food chain. Farmers utilize various agricultural methods aiming at optimizing crop production. However, insufficient understanding of crop nutrient requirements frequently results in the overuse of fertilizers, leading to considerable degradation of soil quality (Sharma et al., 2009; Gupta et al., 2023). While this issue and sources remains unaddressed and its possible reasons was exacerbated by cropping pattern shifts, watershed influences from the Shivalik mountains, and irrigation practices used by farmers. Therefore, the need for soil assessment in the state's district has become imperative to understand and address the impact of these agricultural practices (Shikha et al., 2023). (Haruna and Yahaya, 2021) conducted a study indicating the potential for nutrient accumulation in plants from soil. This is attributed to the inherent ability of plants to transform inorganic forms into diverse organic species, such as bioactive compounds. These compounds can impact the plant and consumer when present in excess and can have significant implications for human nutrition and health. However, when nutrient levels in the soil exceed tolerable limits, it can lead to a toxic nature (Abrahams, 2002). The specific outcome varies depending on the digestibility of various food proteins and the composition of compounds in a given plant. To assess geological samples, conventional analytical techniques are employed, such as wet-chemical methods which require the dissolution of samples through strong acids and often involve intricate procedures, especially when dealing with complex matrix samples. To avoid these destructive, and time consuming methods, more advantageous approaches can be utilized for the analysis of geological samples especially soil. This approach offers benefits such as eliminating reagent blank corrections and reducing sample handling. (Balaram, 2021; Maenhaut, 1992) Other analytical methods are also employed, such as Atomic Absorption Spectroscopy (AAS), Scanning Electron Microscopy Energy Dispersive X-ray (SEM-EDX), and Laser Ablation Inductively Coupled Plasma Mass Spectrometry (LA-ICP-MS) for the chemical characterization of samples (Maenhaut, 1992; Melaku et al., 2005; Lee et al., 2003; Bacon et al., 2023). In addition, Electron Probe Microanalysis (EPMA) and Atomic Emission Spectroscopy (AES) are also used for this purpose (Lee et al., 2003; Yang et al., 2022). As discussed, numerous procedures and techniques exist for determining

soil fertility parameters in the laboratory, while many suffer from analytical challenges and operational inefficiencies. These issues encompass problems related to consistency, dependability, time consumption, and labour intensiveness. As an alternative, using nuclear technology for analysis of soil presents a promising solution. This approach demands minimal sample preparation, offers swifter results, non-destructiveness, and a safe working environment. Moreover, it extends beyond macro and microelements. It simultaneously measures other trace elements, including rare earth elements, heavy elements, transition elements, etc. enhancing its appeal as a comprehensive and efficient method for soil analysis (Sharma et al., 2021). In the realm of nuclear analytical techniques, methods like (Instrumental Neutron Activation Analysis) INAA, Ion Beam Analysis (IBA), Particle Induced X-Ray Emission (PIXE), PIGE, and Prompt Gamma Neutron Activation Analysis (PGNAA) are commonly employed for the analysis of solid samples. Among the different techniques available, both INAA and PGNAA stand out because they minimize matrix effects and offer comprehensive chemical characterization. These methods can simultaneously determine elements across a wide concentration range, from major to trace levels. Nuclear and radio-analytical techniques offer the advantage of depth penetration into the sample due to the high penetration power of neutron and gamma rays (Peng et al., 2022; Verma, 2007). PGNAA and NAA methods deliver bulk sample results. However, IBA techniques, including PIXE and PIGE, are gaining popularity for online measurements of direct or pellet samples, facilitating both qualitative and quantitative analyses (Amonette and Sanders, 1994). The interaction of charged particles with matter in IBA techniques causes nuclear and atomic excitation of the sample's elements. PIGE is excellent for certain isotopes and is particularly proficient in determining the low atomic number ($Z \leq 16$) elements, such as Boron, Lithium, Fluorine, Sodium, Aluminum, Magnesium, Silicon, Phosphorus, and Sulfur (Dhorge et al., 2017; Samanta et al., 2020). It measures prompt gamma rays produced by inelastic scattering and nuclear reactions. In contrast, PIXE determines medium to high atomic number ($Z > 15$) elements. For a comprehensive analysis of direct samples in powder form and the simultaneous determination of numerous trace-level elements, highly sensitive techniques like INAA are indispensable.

INAA methods entail irradiating the sample using high-flux neutrons. They can able to quantify from low to medium and high atomic number elements (likely Na to Th), including transition elements and Rare Earth Elements (REEs) etc. with exceptional sensitivity and low detection limits using high-resolution gamma-ray spectrometry with HPGe detectors (Chambhare et al., 2021; El-Taher, 2018). In this study, we apply nuclear analytical techniques (INAA), ion beam methods (PIGE), and X-ray fluorescence methods: ED-XRF (Custo et al., 2005) to assess the soil quality and composition of arable lands in the Hoshiarpur region of Punjab. Our analysis covers 26 elements, including major, minor, and trace elements, aiming to understand potential environmental health implications. This comprehensive approach ensures a detailed exploration of soil characteristics, maintaining clarity and uniqueness in our research.

Sample sites

Hoshiarpur District showcases an alluvial plain as its prominent physiographic unit, nourished by the Beas and Sutlej Rivers, with significant drainage systems. The district witnesses an average annual rainfall of 938 mm, with variations in distribution and irrigation in this region primarily relies on rainfall, Tube wells and canal networks. The Shivalik mountain range flanks the district to the northeast, influencing the region's overall climate and natural habitat. The geological map of Punjab highlighting Hoshiarpur is shown in Fig. 1 with the sampling locations. The samples were taken from agricultural soil of different villages of the district. The chosen 22 sites were deliberately selected to reflect regions characterized by comparable cropping practices typical among local farmers. Differences between these sites are probably due to variations in farmers' use of different fertilizers and individual application practices. Disparities among the chosen sites were predominantly linked to variations in fertilizer types and quantities utilized on a per-hectare basis.

Sample collection and preparation

The uppermost layer of soil, or topsoil, was collected from a depth of 10 to 15 cm. After removing organic debris and vegetation, 22 soil samples were

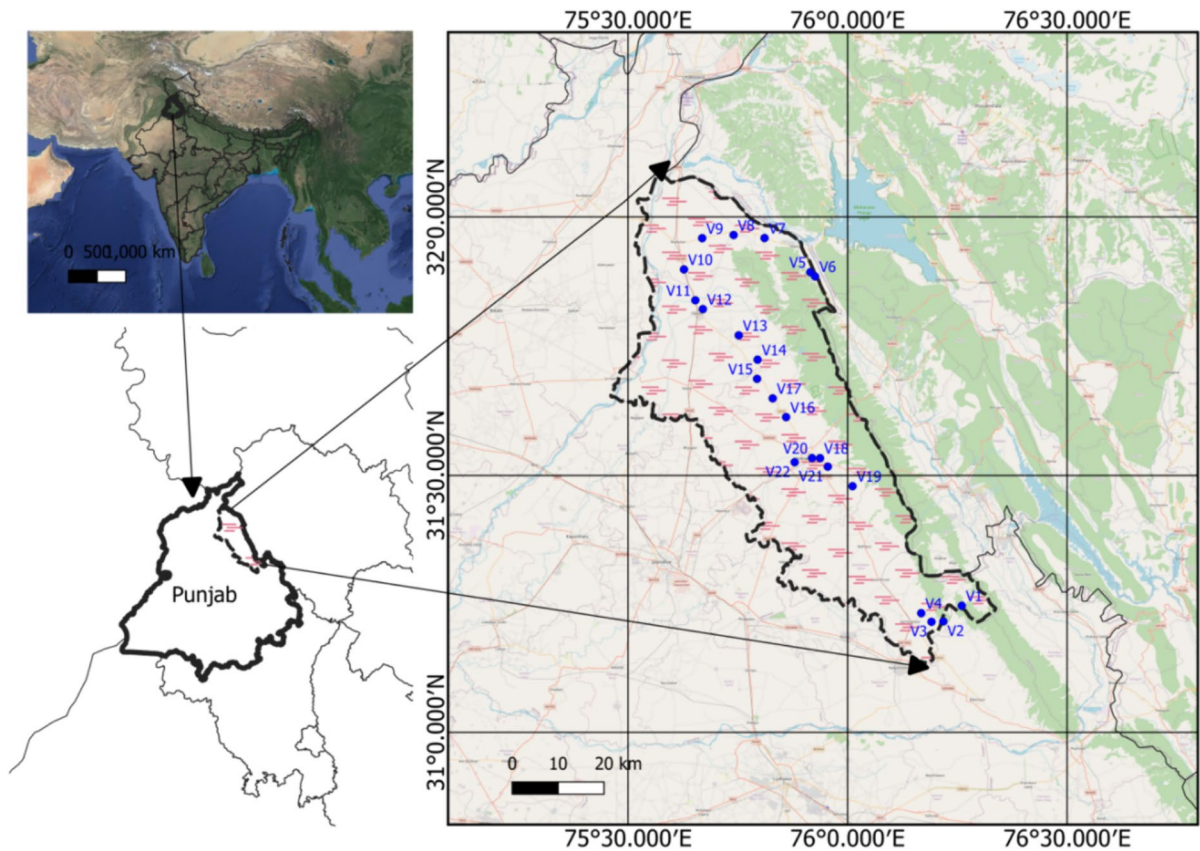


Fig. 1 Illustrates the visual representation of the study area map

obtained using a spatula and V-shaped sampling. The samples were sun-dried, crushed into fine particles, and oven-dried at 105 °C for 14 h until a constant weight was reached. They were sieved through a 1.5 mm mesh for uniformity and sealed in labeled zip-lock polythene bags. Along with study area visual representation, the details of sample collection was tabulated (Table 1). In this region, the predominant land use system involved growing a mixture of food and fodder crops. The primary food crops cultivated include maize (*Zea mays* L.), wheat (*Triticum aestivum* L.) and fodder crop was barley (*Hordeum vulgare* L.), sorghum (*Sorghum bicolor* L.). The selected soil samples in this study involving food crop cultivation and almost all farmers predominantly use chemical fertilizers, such as nitrogen-based urea and Diammonium Phosphate (DAP). The samples that were collected over the

past several decades exhibit a consistent cropping pattern, with the same described crop cycle.

Materials and methods

INAA

Irradiation was conducted using the pneumatic carrier facility (PCF), with the samples weighing approximately 6 mg, additionally, a self-serve facility (SSF) was employed, with the samples weighing around 75 mg (Acharya and Pujari, 2019). Along with the samples, geological certified reference materials were also irradiated in an identical manner. In the case of PCF, the irradiation procedure involved neutron flux of $\sim 10^{13}$ neutrons per square centimetre per second subjecting bunch of soil samples and certified reference materials (packed inside

Table 1 Description of sample collection, Fertilizers used and crop cycle from different villages of Hoshiarpur district

Sampling code	Name of Village	Latitude	Longitude	Fertilizers used	Crop type
V-1	Rattanpur	31°14'47.7"	76°15'36.9"	DAP + Urea + Gobar Khad	Food crop
V-2	Kunail	31°12'57.8"	76°13'05.6"	DAP + Urea + Gobar Khad	Food crop
V-3	Saddarpur	31°12'55.0"	76°11'28.8"	DAP + Urea	Food crop
V-4	Birampur	31°13'55.8"	76°10'04.4"	DAP + Urea + Potash	Food crop
V-5	Bathehar	31°53'35.7"	75°54'54.8"	DAP + Urea	Food crop
V-6	Bringli	31°53'05.5"	75°55'34.1"	DAP + Urea	Food crop
V-7	NamoliHar	31°57'33.2"	75°48'39.7"	DAP + Urea	Food crop
V-8	Sandhwal	31°57'54.3"	75°44'26.2"	DAP + Urea + Potash	Food crop
V-9	Patial	31°57'32.3"	75°40'08.4"	DAP + Urea + Zn	Food crop
V-10	PindSahibka	31°53'54.7"	75°37'39.1"	DAP + Urea + Potash	Food crop
V-11	Manak,	31°50'19.7"	75°39'12.1"	DAP + Urea	Food crop
V-12	Dasuya	31°49'18.6"	75°40'13.9"	SSP + Urea	Food crop
V-13	Bahtiwala	31°46'15.5"	75°45'08.0"	DAP + Urea + Gobar Khad	Food crop
V-14	Sehjowal	31°43'25.9"	75°47'42.4"	DAP + Urea + Potash + Zinc	Food crop
V-15	Abowal	31°41'12.3"	75°47'38.4"	Urea + DAP + Gobar Khad	Food crop
V-16	Adamwal	31°36'45.1"	75°51'36.4"	DAP + Urea + Gobar Khad	Food crop
V-17	Hazipur	31°38'56.0"	75°49'46.6"	SSP + Urea + Gobar Khad + Potash	Food crop
V-18	Hoshiarpur-1	31°32'00.5"	75°56'14.8"	DAP + Urea + Potash + Zinc	Food crop
V-19	Bassi	31°28'44.8"	76°00'41.3"	DAP + Urea	Food crop
V-20	Gopal	31°32'00.8"	75°55'08.9"	DAP + Urea + Potash + Gobar Khad	Food crop
V-21	Bajwara	31°31'01.2"	75°57'18.4"	SSP + Urea + Gobar Khad	Food crop
V-22	Hoshiarpur-2	31°31'02.4"	75°57'16.3"	DAP + Urea + Gobar Sulphur + Potash Khad	Food crop

a high density polypropylene capsule) for 1 min irradiation to achieve the desired level of activation for analysis of short-lived (sec to min) radioisotopes. Following irradiation, the samples and certified reference materials underwent repackaging and re-weighing and were subsequently mounted on a Perspex plate for short counting (around 1 min) followed by 1 h cooling and recounted for medium-lived isotopes (About ~ 30 min) (Acharya and Pujari, 2019). In self-serve, each sample (soil samples and certified reference materials) was individually enveloped in pure aluminium foil, ensuring separation, and subjected to co-irradiation within a sealed aluminium can for a duration of 4 h. This procedure occurred at the Dhruva research reactor, boasting a flux of approximately 10^{13} neutrons per square centimetre per second. Following an appropriate cooling period exceeding four days, the samples and reference materials underwent cleaning (to restore all its sample mass) from old aluminium sheet which was irradiated and the samples were again wrapped in new aluminum foil to avoid

unwanted peaks originated from aluminium sheet. The freshly wrapped samples was placed on a Perspex plate, ensuring consistent detector geometry to minimize the error during counting of gamma rays. The characteristic gamma rays emitted by the activation products of the respective analytes from both PCF and SSF were measured using a 40% relative efficiency high-purity germanium detector (HPGe) coupled to a PC-based 4 k Multi-Channel Analyzer (MCA). The analysis of peak areas was conducted with precision using the peak-fit method through the utilization of the Pulse Height Analysis Software (PHAST), an innovative tool developed at BARC. A typical gamma-ray spectrum of a soil sample subjected to neutron irradiation in the research reactor is illustrated in Figs. 2 and 3, utilizing INAA (SSF and PCF), respectively. The relative method determined the elemental concentrations for both facilities in the samples. This involved comparing the decay-corrected count rates of the samples to the count rates of standard reference materials, as

Fig. 2 Typical gamma-ray spectra of soil sample after 1 min irradiation by neutron beam

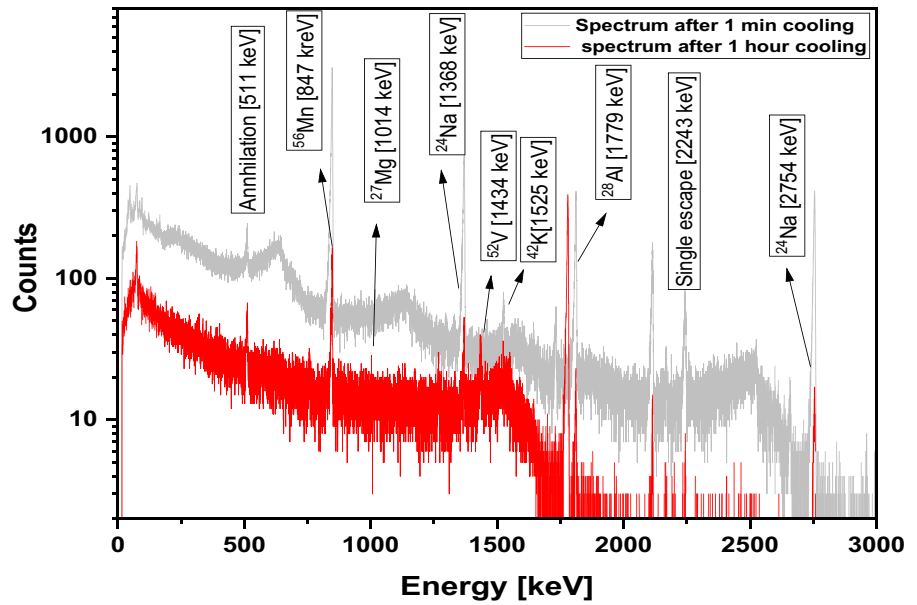
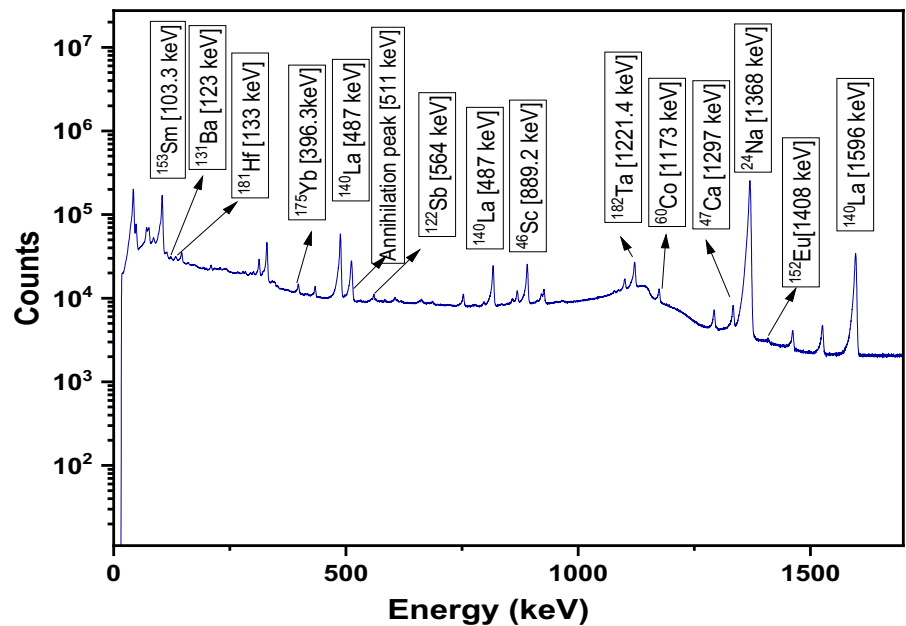


Fig. 3 The typical gamma-ray spectrum of the soil sample utilizing self-serve facility



expressed in the following equation (Sharma et al., 2022):

$$m_{x, sample} = m_{std} \cdot \frac{cps_{x, sample}}{cps_{x, std}} \cdot \frac{D_{std}}{D_{sample}} \quad (1)$$

Here, 'm_{x, sample}' represents the mass of a specific element in the sample for elemental analysis, 'm_{std}' is

the mass of the standard, cps denotes counts per second for the standard and sample gamma rays respectively i.e. cps_{x, sample} and cps_{x, std}, while 'D' represents the decay constant for the particular element in sample and standard i.e. D_{sample} and D_{std} respectively. The decay constant is crucial for adjusting the impact of radioactive decay on the elements.

The absolute elemental mass of the element in the sample was then converted to relative concentration, estimated in units, namely mg/kg and % (by wt), which was achieved by dividing it by the total sample mass. Figures 2 and 3 illustrate a representative gamma-ray spectrum obtained from a soil sample using PCF and SSF, respectively. Upon irradiating the soil sample, we estimated the elements, namely Na, Al, Mg, V, Mn and K. After irradiating the sample for about 4 h (utilizing SSF), almost 12 elements were identified, including REEs and other trace elements namely Co, Ta, Na, Ca, Hf, Ba, Sb, Sc, Eu, La, Sm and Yb.

IBA (PIGE)

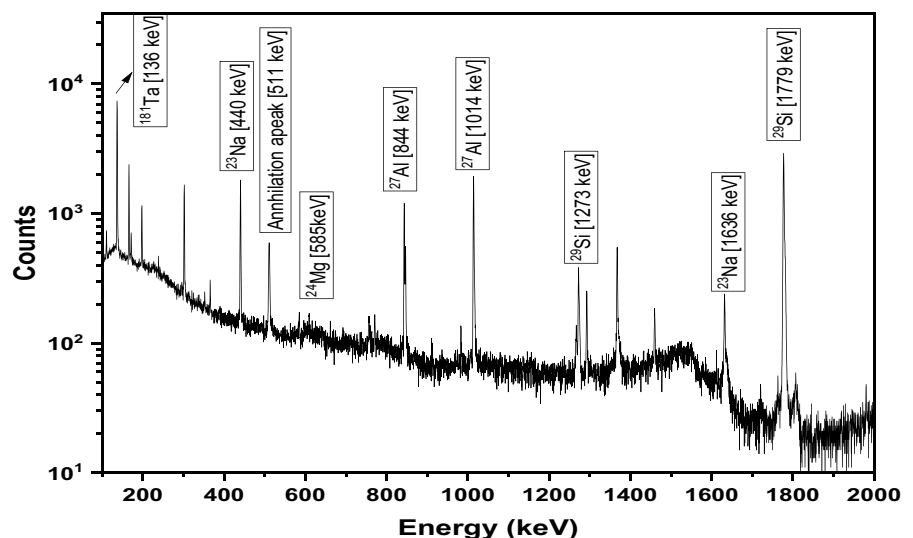
The PIGE experiment utilized a 5 MeV proton beam from the Folded Tandem Ion Accelerator (FOTIA), BARC, directed through the beam line into one side of the vacuum chamber. Thin tantalum achieved the beam cut-off energy at 1.25 MeV, and the final beam energy right after the exit window reached 3.75 MeV. For optimal focusing, a tantalum collimator with a 2 mm aperture was positioned on the exit side of the window, concentrating the proton beam to a size of 2 mm. The target, comprising a soil sample or reference material, was affixed to the tantalum collimator (2 mm) and subjected to irradiation using a 3.75 MeV proton beam with a current of approximately ~7 nA. A 40%, relative efficiency

HPGe detector was used to measure the characteristic prompt gamma-rays at a 90° angle to the beam direction. Throughout the experiment, fluctuations in beam current were monitored by assessing the count rate of the 135 keV gamma line from ¹⁸¹Ta (the window material). Quantification of four elements, namely Si, Na, Al, and Mg was achieved through their characteristic gamma lines derived from (p, p'γ) inelastic scattering reactions: ²⁸Si (p, p'γ) ²⁸Si; ²³Na (p, p'γ) ²³Na; ²⁷Al (p, p'γ) ²⁷Al, and ²⁵Mg (p, p'γ) ²⁵Mg, utilizing their respective intensities at 1779 keV, 440 keV, 1014 keV, and 585 keV. Figure 4 illustrates a representative prompt gamma-ray spectrum obtained from a soil sample using the external (in air) PIGE setup. In order to quantify elements, USGS AGV-1 and USGS RGM-1 geological certified reference materials were packed similarly. In this work, the total concentrations in the sample were determined by relative method. The sample concentrations were determined by the following calculation shown in Eq. 2 (Raja and Acharya, 2023).

$$C_{x, sample} = \frac{CPS_{x, sample}}{CPS_{x, std}} \cdot \frac{(CPS_{Ta})_{std}}{(CPS_{Ta})_{sample}} \times C_{x, std} \tag{2}$$

where “C_{x, sample}” is the sample’s elemental concentration, and CPS is the count rate of the analyte in the standard sample. i.e. CPS_{x, std}, in sample i.e. CPS_{x, sample} and in Tantalum window i.e. “(CPS_{Ta})” is the count rate of Ta at 136 keV during irradiation of standard material and sample i.e. (CPS_{Ta})_{std} and (CPS_{Ta})_{sample}.

Fig. 4 Typical gamma-ray spectrum of a soil sample in the external PIGE method (in the air) using a ~3.5 MeV proton beam



“ $C_{x, \text{std}}$ ” is the known standard elemental concentration for a particular analyte. The typical prompt gamma-ray spectrum as illustrated in Fig. 4 after the sample is irradiated by a proton beam of energy 3.75 MeV.

ED-XRF

In the context of Energy Dispersive X-ray Fluorescence -ED-XRF, the samples and standards (each weighted 200 gm) underwent irradiation employing X-rays (emission current = 100 mA) sourced from Rhodium (Rh) with a maximum energy of 40 keV, and this process of irradiation was sustained for 100 s. The X-rays emitted from the target material were subsequently measured using a Silicon Lithium detector. The selection of peak areas for both the sample and standard was executed using the built-in software (Custo et al., 2005). The typical

X-ray spectrum of soil samples utilizing the energy-dispersive X-ray technique is shown in Fig. 5. The elements estimated via this technique were Ti, Fe, Ca, Mn, Cr, Rb, Sr, Zr, Pb and Zn. The uncertainties were represented as total combined propagated uncertainties. These uncertainties, primarily influenced by errors in mass measurement and counting statistics of both the sample and elemental standard, and a set of 10 standard reference materials including Soil-5, SY 2, AGV-1, PCC, RGM, ECH, EOP, NIES, MRG-1, and SL-1 were employed to assess the concentrations of 10 elements (Ca, Ti, Fe, Mn, Rb, Sr, Cr, Pb, Zn, & Zr).

Evaluation of ecological risk assessment

Heavy metal (HMs) contamination in soil can be effectively assessed by key indices such as Contamination Factor (CF), Potential Ecological Risk

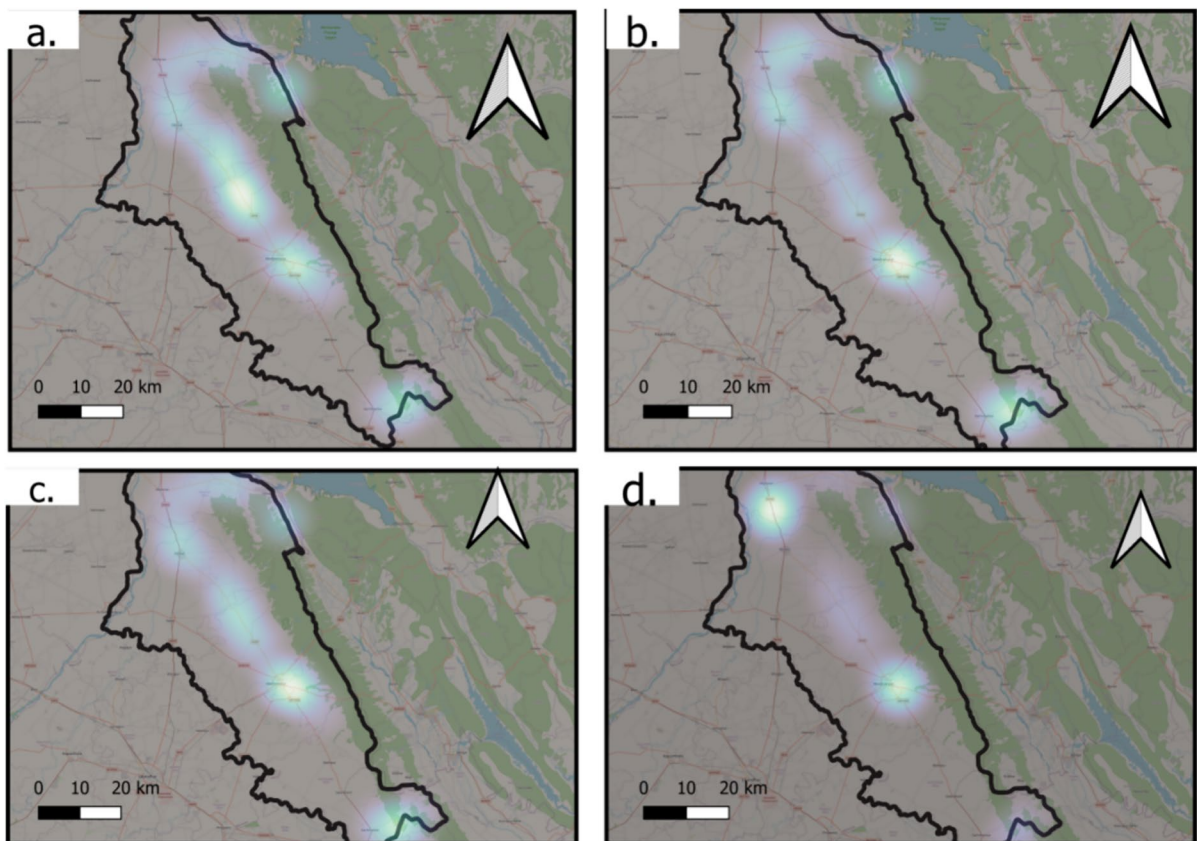


Fig. 5 Heat maps of **a** Yb, **b** Sm, **c** La, and **d** Eu at the study area sites

Index (PERI), Pollution load index (PLI) and Geo-accumulation factor (I_{geo}) (Esen et al., 2024). These indices offer a comprehensive understanding of ecological sensitivity, concentration levels, and toxicity of HMs in the arable soil environment.

CF is a metric for assessing soil pollution. It can be calculated as:

$$CF = \frac{C_n}{C_b} \tag{3}$$

where C_n represents the element concentration in the soil sample, and C_b is the geochemical background value in uncultivated soil within the study region; soil quality categorization was determined by the Contamination Factor (CF). The CF values signify contamination levels: $CF < 1$ indicates low contamination, $1 \leq CF < 3$ suggests moderate contamination, $3 \leq CF < 6$ signifies considerable contamination, and $CF \geq 6$ reflects very high contamination.

The potential ecological risk index associated with each metal element can be calculated using the following formula:

$$PERI = \frac{C_s}{C_n} \times T_r \tag{4}$$

C_s represents the elemental concentration in the soil sample, C_n is the geochemical background value of unaffected soil of the study area region, and T_r denotes the toxic response factor specific to each metal.

The toxic-response factors for heavy metals are Mn, Zn=1, Pb, Co=5 and Cr=2 (Taiwo et al., 2019). Soil quality classification based on the PERI value was delineated as follow: $PERI < 40$ indicates low risk, $40 \leq PERI < 80$ signifies moderate risk, $80 \leq PERI < 160$ indicates considerable risk, $160 \leq PERI < 320$ reflects high risk, and $PERI \geq 320$ represents very high risk.

The pollution load index represents the number of times by which the toxic element concentrations in the sediment exceed the background concentration and gives a summed indication of the overall level of pollution status in a particular sample. For the entire sampling site, PLI has been estimated by the n-root from the product of n CFs of the studied elements included:

$$PLI = (CF1 \times CF2 \times CF3 \times \dots \times CFn)^{\frac{1}{n}} \tag{5}$$

The index permits a simple, comparative means for assessing pollution levels. A PLI of > 1 is contaminated, whereas < 1 indicates un-contaminated site.

Four rare earth elements, namely Yb, Sm, La, and Eu, were detected upon analyzing the agricultural soils of 22 locations in the Hoshiarpur district. The I_{geo} index was calculated to assess their accumulation on the topsoil of agricultural soil utilizing Eq. 3 (Muller, 1969).

$$I_{geo} = \text{Log}_2 \left(\frac{C_n}{B_n \times 1.5} \right) \tag{6}$$

The specific elemental concentration in the topsoil, denoted as C_n , as compared to the corresponding concentrations of elements in the upper continental crust (UCC), represented as B_n , as shown in Table 2. Adding the constant 1.5 in the equation facilitated the exploration of natural environmental variations.

For assessment of contamination, I_{geo} values above 5 indicate extreme pollution, 4–5 signify high pollution to extreme pollution, 3–4 indicate moderate to high pollution, and 2–3 denote moderate pollution to high pollution. I_{geo} values 1–2 categorize sediment/ soil as moderately polluted, while an I_{geo} value 0 implies unpolluted to moderately contaminated condition. An I_{geo} value of ≤ 0 indicates the natural baseline concentration which is not contaminated,

Results and discussion

To validate our methodology and ensure reliability of the reported results geological certified reference materials (CRMs) such as USGS RGM-1 and USGS AGV-1 were used. The accuracy was affirmed by

Table 2 Standard reference value of rare earth elements used in this work

Element	Upper continental crust (UCC) (in mg/kg ⁻¹)
Yb	2.2
Sm	4.5
La	30
Eu	0.88

analyzing the Geological CRM, RGM-1, as a control sample, along with the matrix-matched AGV-1as a reference material.

A total of twenty-six elements were identified using three methods: ED-XRF, PIGE, and INAA (SSF& PCF). ED-XRF determined 10 elements, comprising 4 major (Ca, Ti, Fe, & Mn) and 6 minor (Rb, Sr, Cr, Pb, Zn, & Zr) elements. Ion beam analysis (IBA), specifically PIGE, identified 4 elements, namely Si, Na, Mg, and Al. Meanwhile, INAA (PCF, SSF) demonstrated capability in determining 20 elements across major, minor, and trace concentration levels, including Yb, Sm, La, Eu, Sc, Sb, Ba, Hf, Ca, Na, Ta, Sc, Co, Al, Mg, Ca, V, Na, Mn, and K.

The Z-score acts as a measure of how many standard deviations a given concentration deviates from the population mean. It is calculated within a 95.5% confidence interval and is expressed by the formula:

$$Zscore = \frac{X - \mu}{\sigma} \quad (7)$$

where the expression "X" represents the average value measured in a laboratory, 'μ' denotes the mean of the entire population, and 'σ' represents the overall uncertainty in the population.

Magnitude of Z-scores are categorized as:

When $|Z| < 1$; Results are considered as good.

$1 \leq |Z| \leq 2$; Results are acceptable.

$2 \leq |Z| \leq 3$; Results are questionable and deemed unacceptable.

The Z-score values calculated for PIGE and INAA (SSF & PCF) were determined to be within the range of ± 2 , indicating satisfactory precision and accuracy, with the exception of Mg, which showed a Z-score of ~ -3.19 as shown in Table 3.

The precision and accuracy in this study are quantified through the use of relative standard deviations

Table 3 Elemental concentration of USGS AGV-1, their officially certified values, relative standard deviation % and the Z-scores employing INAA (SSF and PCF) and PIGE technique (concentration in mg/kg otherwise indicated)

Sr no	Element	Technique	Energy (keV)	Certified reference value	Obtained value	Z score	RSD%
1	Yb	INAA-SSF	396.3	2.60 ± 0.30	5.20 ± 0.86	-1.54	6.5
2	Sm	INAA-SSF	103.2	4.33 ± 0.30	5.21 ± 0.50	-0.90	2.6
3	La	INAA-SSF	1596	24.0 ± 1.1	22.0 ± 1.5	0.60	4.5
4	Eu	INAA-SSF	121.8	0.66 ± 0.08	0.87 ± 0.11	-0.91	7.6
5	Sc	INAA-SSF	889.2	4.40 ± 0.30	6.20 ± 0.67	-1.40	5.3
6	Sb	INAA-SSF	564	1.30 ± 0.10	0.80 ± 0.10	2.31	6.0
7	Ba	INAA-SSF	123.8	810 ± 46	635 ± 37	2.30	5.5
8	Hf	INAA-SSF	133	6.20 ± 0.30	9.22 ± 0.85	-1.77	7.9
9	Ca	INAA-SSF	159	8210 ± 500	9740 ± 657	-1.18	9.8
10	Na	INAA-SSF	1368.6	31,600 ± 100	30,850 ± 1420	0.23	1.7
11	Ta	INAA-SSF	1121	0.95 ± 0.10	1.62 ± 0.24	-1.48	12.4
12	Sc	INAA-SSF	1120.5	4.40 ± 0.30	6.20 ± 0.67	-1.40	10.0
13	Co	INAA-SSF	1332	2.00 ± 0.20	3.50 ± 0.45	-1.71	7.6
14	Na(%)	PIGE	440	3.16 ± 0.01	3.19 ± 0.09	-0.09	0.8
15	Al(%)	PIGE	1014	8.33 ± 0.18	8.85 ± 0.82	0.94	7.2
16	Si(%)	PIGE	1273	27.46 ± 0.84	28.13 ± 1.87	-1.45	1.8
17	Mg(%)	PIGE	585	1.02 ± 0.06	1.25 ± 0.1	-2.80	7.0
18	Al	INAA-PCF	1778	83,300 ± 1800	81,150 ± 1510	-1.20	2.0
19	Mg	INAA-PCF	843	10,200 ± 600	8280 ± 830	-3.19	15.8
20	Ca	INAA-PCF	3085	8210 ± 500	9930 ± 335	-0.14	10.0
21	V	INAA-PCF	1434	102 ± 12	107 ± 20	0.41	5.8
22	Na	INAA-PCF	2754	31,600 ± 100	30,800 ± 1420	0.27	1.9
23	Mn	INAA-PCF	846	880 ± 60	880 ± 94	-0.02	1.2
24	K	INAA-PCF	1525	27,200 ± 800	28,220 ± 632	1.27	2.0

(% RSD) and Z scores, respectively. The % RSD values were observed to exhibit variation across different elements and can be computed using the formula:

$$\text{Relative standard deviation} = \frac{s}{|X|} \tag{8}$$

where s=sample standard deviation and |X|=sample mean.

The % RSD values for PIGE results were determined as follows: Na (~0.8%), Al (~7.2%), Mg (~7%), and Si (~1.8%). Notably, INAA exhibited satisfactory accuracy and precision, with relative errors for all identified elements consistently below <10% (Table 3), except for Ta, Sc, Mg, and Ca in the geological standard reference material (AGV-1).

In the ED-XRF analysis, a set of 10 standard reference materials—Soil-5, SY 2, AGV-1, PCC, RGM, ECH, EOP, NIES, MRG-1, and SL-1 were employed to assess the concentrations of 10 elements (Ca, Ti, Fe, Mn, Rb, Sr, Cr, Pb, Zn, &Zr). Each standard weighed ~200 gm and was irradiated by electron beam generated by Rhodium source. Figure 5 showed

graphs plotting normalized counts against elemental concentrations, using specified standards to measure multiple elements.. To evaluate the accuracy of this method, R-square values were reported for all 10 elements. Notably, coefficient exceeded 0.9, indicating high accuracy in the analysis.

INAA (PCF and SSF), PIGE, and ED-XRF analysis determined elemental concentrations in soil samples. The results are reported in mg kg⁻¹ or % by weight, as shown in Tables 4, 5, 6 and 7 respectively. These concentrations was are also compared with global values to provide context regarding the elemental composition of the soil with the mean elemental concentrations (in Table 8).

The heat maps for all the estimated rare earth elements are shown in Fig. 5, indicating the accumulation at the sites using the I_{geo} index. Table 9 shows that Eu does not show any significant accumulation in the agricultural field, as the accumulation factor ranges between -0.51 and 1.86. However, the remaining REEs; La, Sm and Yb, have means corresponding to accumulation factors of 9.7, 6.06 and 5.5,

Table 4 Determined elemental concentrations (in mg kg⁻¹, otherwise indicated) for soil samples by INAA-PCF

Sample ID	Al(% by wt)	Mg (% by wt)	Ca(% by wt)	V	Na(% by wt)	Mn	K((% by wt)
V-1	3.64±0.04	0.19±0.07	0.95±0.04	20.6±2.3	1.55±0.03	529.71±43.11	2.46±0.08
V-2	4.11±0.04	0.26±0.10	0.90±0.03	29.2±3.3	1.22±0.02	656.07±53.40	5.13±0.18
V-3	2.72±0.03	0.12±0.04	0.85±0.03	22.6±2.6	1.21±0.02	454.98±37.03	3.35±0.11
V-4	4.92±0.05	0.26±0.10	0.74±0.03	170.2±19.6	1.93±0.04	791.31±64.41	2.88±0.10
V-5	5.25±0.06	0.23±0.09	0.81±0.03	99.1±11.4	1.19±0.02	830.22±67.57	2.46±0.08
V-6	4.55±0.05	0.14±0.05	0.80±0.03	72.9±8.4	1.02±0.02	804.12±65.45	2.77±0.09
V-7	1.60±0.01	0.04±0.01	1.15±0.05	60.5±6.9	2.54±0.05	683.29±55.61	3.39±0.12
V-8	8.70±0.10	0.12±0.05	0.51±0.02	42.4±4.8	1.83±0.04	283.97±23.11	2.90±0.10
V-9	4.74±0.05	0.13±0.05	0.42±0.01	31.8±3.6	1.32±0.03	642.91±52.33	3.34±0.11
V-10	3.72±0.04	0.12±0.05	0.67±0.03	15.4±1.7	1.31±0.03	1179.42±96.00	2.5±0.08
V-11	4.12±0.04	0.20±0.07	0.64±0.02	21.7±2.5	1.46±0.03	792.75±64.52	2.75±0.09
V-12	3.41±0.03	0.17±0.06	0.66±0.02	27.1±3.1	1.56±0.03	633.19±51.54	2.45±0.08
V-13	4.33±0.05	0.18±0.07	0.55±0.02	23.6±2.7	1.34±0.03	866.36±70.52	2.64±0.09
V-14	3.81±0.04	0.13±0.05	0.50±0.02	13.2±1.5	1.64±0.03	761.42±61.97	2.75±0.09
V-15	2.44±0.02	0.12±0.05	0.51±0.02	18.8±2.1	1.27±0.02	845.14±68.79	2.62±0.09
V-16	3.14±0.03	0.20±0.08	0.91±0.04	16.6±1.9	1.48±0.03	1132.91±92.21	2.69±0.09
V-17	3.21±0.03	0.21±0.08	1.00±0.04	22.3±2.5	1.50±0.03	940.05±76.52	2.51±0.08
V-18	3.64±0.04	0.15±0.06	0.85±0.03	17.9±2.0	1.33±0.03	1035.37±84.27	3.03±0.10
V-19	3.21±0.03	0.23±0.09	0.90±0.03	14.4±1.6	1.67±0.03	831.72±67.70	2.98±0.10
V-20	2.75±0.03	0.17±0.07	0.85±0.03	26.8±3.0	1.61±0.03	1049.25±85.40	2.87±0.10
V-21	4.15±0.04	0.24±0.09	0.85±0.03	28.1±3.2	1.42±0.03	1146.7±93.34	2.53±0.09
V-22	3.84±0.04	0.04±0.01	0.89±0.03	19.2±2.2	1.67±0.03	1132.91±92.21	2.44±0.08

Table 5 Determined elemental concentrations (in mg kg⁻¹, otherwise indicated) for soil samples by INAA-SS

Sample ID	Co (% by wt)	Yb	Sm	La	Eu	Sc	Sb	Ba	Hf	Na (% by wt)	Ta
V-1	1.84±0.07	15.19±0.77	11.41±0.81	39.26±1.85	3.59±0.44	21.84±1.40	0.53±0.05	1084±22	53.33±2.64	1.08±0.03	0.33±0.03
V-2	1.24±0.05	21.16±1.08	22.01±1.50	83.78±3.32	3.739±0.4	14.08±0.84	0.47±0.04	1250±32	42.12±2.08	1.25±0.04	0.24±0.02
V-3	1.84±0.07	15.19±0.75	11.41±0.79	39.26±0.31	BDL	21.84±1.54	0.44±0.03	1142±14	53.33±2.64	1.14±0.03	0.33±0.03
V-4	23.05±0.69	3.23±0.16	27.7±1.89	28.23±0.91	1.20±0.147	11.92±0.66	BDL	1402±47	54.4±2.69	1.40±0.04	BDL
V-5	1.31±0.03	26.52±1.51	23.72±1.61	10.60±0.12	BDL	18.14±1.08	0.61±0.06	1368±16	62.72±3.1	1.37±0.04	0.44±0.04
V-6	1.44±0.06	28.42±1.90	29.64±2.07	34.21±0.31	BDL	23.35±1.38	0.39±0.03	3817±30	58.68±2.9	3.82±0.11	0.39±0.03
V-7	4.06±0.12	84.37±4.40	BDL	334.37±1.91	BDL	63.31±3.78	1.11±0.11	951±20	202±10	0.95±0.03	1.02±0.05
V-8	1.81±0.05	17.18±0.85	11.39±0.77	41.30±0.51	3.21±0.39	19.55±1.14	0.46±0.04	1248±35	57.04±2.82	1.25±0.04	0.51±0.05
V-9	23.07±0.70	26.85±1.30	278.2±19.4	26.42±0.76	2.50±0.30	14.29±0.84	0.54±0.05	1138±28	61.22±3.02	1.14±0.03	0.42±0.04
V-10	1.87±0.07	17.18±0.15	23.61±1.61	12.01±0.12	6.24±0.75	21.72±1.26	0.33±0.02	1410±42	45.81±2.27	1.41±0.04	0.31±0.03
V-11	1.46±0.06	24.70±1.22	30.08±2.14	36.02±0.41	4.51±0.55	11.67±0.66	0.52±0.05	1372±18	64.93±3.22	1.37±0.04	BDL
V-12	1.88±0.05	17.18±0.85	29.85±2.01	281.58±1.43	1.24±0.14	18.43±1.08	0.57±0.06	3855±50	47.96±2.37	3.86±0.12	0.46±0.04
V-13	1.36±0.04	96.66±0.66	11.38±0.65	33.83±0.85	3.04±0.41	22.99±1.37	0.49±0.03	956±22	55.08±2.73	0.96±0.03	0.49±0.04
V-14	1.16±0.03	17.14±0.85	21.9±1.55	25.92±1.52	3.20±0.39	62.81±3.76	0.48±0.04	1255±33	48.87±2.42	1.26±0.04	0.41±0.04
V-15	4.10±0.12	102.03±11.80	BDL	312.77±1.76	3.06±0.44	20.19±1.26	0.41±0.04	1145±26	52.11±2.58	1.15±0.03	1.01±0.05
V-16	1.25±0.03	17.18±0.12	11.37±0.61	41.56±0.51	BDL	14.87±0.89	1.05±0.1	1395±45	203.5±10.8	1.40±0.04	0.36±0.03
V-17	1.11±0.03	123.51±6.30	27.7±1.80	68.59±2.72	BDL	22.12±1.35	BDL	1350±15	59.39±2.94	1.35±0.04	0.28±0.02
V-18	5.01±0.15	112.77±5.60	23.53±1.61	12.64±0.98	BDL	11.34±0.68	0.43±0.04	3802±40	44.27±2.2	3.80±0.11	0.47±0.04
V-19	1.33±0.03	48.33±2.63	BDL	19.88±1.22	1.31±0.15	19.89±1.19	0.35±0.03	960±24	54.67±2.71	0.96±0.03	0.38±0.03
V-20	22.99±0.68	59.07±2.88	BDL	47.62±0.62	BDL	23.71±1.42	0.38±0.03	1230±36	56.75±2.81	1.23±0.04	1.06±0.05
V-21	1.40±0.04	21.48±1.51	BDL	91.83±3.64	BDL	63.99±3.78	0.42±0.04	1125±25	61.98±3.07	1.13±0.03	0.45±0.04
V-22	1.11±0.003	85.92±4.25	BDL	10.21±0.09	BDL	20.67±1.20	0.31±0.03	1425±49	202.1±10.1	1.43±0.04	0.51±0.05

Table 6 Elemental concentrations (mg kg⁻¹/% by wt as indicated) for soil samples by utilizing the PIGE technique

Sample ID	Si (% by wt)	Na % by wt)	Mg (% by wt)	Al (%by wt)
V-1	30.98 ± 0.77	1.26 ± 0.20	0.18 ± 0.004	3.50 ± 0.10
V-2	29.76 ± 0.67	1.41 ± 0.22	0.22 ± 0.006	4.20 ± 0.13
V-3	32.71 ± 0.72	1.28 ± 0.20	0.13 ± 0.003	2.81 ± 0.08
V-4	34.56 ± 0.94	1.39 ± 0.22	0.22 ± 0.006	5.12 ± 0.15
V-5	29.28 ± 0.76	1.11 ± 0.17	0.24 ± 0.005	5.11 ± 0.15
V-6	27.21 ± 0.77	1.09 ± 0.17	0.13 ± 0.003	4.41 ± 0.13
V-7	26.07 ± 0.70	1.11 ± 0.17	0.12 ± 0.002	1.82 ± 0.05
V-8	31.77 ± 0.78	1.20 ± 0.19	0.12 ± 0.003	1.41 ± 0.03
V-9	30.38 ± 0.74	1.04 ± 0.16	0.11 ± 0.003	4.51 ± 0.13
V-10	23.30 ± 0.61	1.03 ± 0.16	0.11 ± 0.003	4.46 ± 0.12
V-11	33.51 ± 0.81	1.21 ± 0.19	0.27 ± 0.007	4.14 ± 0.12
V-12	30.71 ± 0.69	1.26 ± 0.20	0.16 ± 0.004	3.32 ± 0.10
V-13	28.97 ± 1.88	1.01 ± 0.16	0.21 ± 0.005	4.21 ± 0.13
V-14	25.28 ± 0.59	1.15 ± 0.18	0.13 ± 0.003	3.54 ± 0.10
V-15	30.24 ± 0.66	1.01 ± 0.16	0.14 ± 0.003	2.51 ± 0.07
V-16	37.16 ± 0.82	1.57 ± 0.25	0.14 ± 0.003	3.10 ± 0.09
V-17	31.83 ± 0.74	1.01 ± 0.16	0.16 ± 0.004	3.50 ± 0.10
V-18	31.28 ± 0.72	1.27 ± 0.20	0.17 ± 0.004	3.60 ± 0.11
V-19	26.62 ± 0.66	1.09 ± 0.17	0.21 ± 0.005	3.14 ± 0.09
V-20	27.62 ± 0.70	1.02 ± 0.16	0.13 ± 0.003	2.74 ± 0.08
V-21	27.12 ± 0.69	1.03 ± 0.16	0.10 ± 0.002	4.21 ± 0.13
V-22	30.24 ± 0.74	0.95 ± 0.15	0.08 ± 0.002	3.52 ± 0.10

with uncertainty of 1.45, 1.05 and 1.30, respectively, which shows serious contamination of rare earth elements, in arable soils of Hoshiarpur.

From Fig. 5 it can be seen that for Yb, the most significant accumulation was observed in Hazipur (V-17) and Hoshiarpur (V-18), followed by other locations. Patial (V-9) exhibited the highest concentration of Sm. Namoli-Har(V- 7) showed the highest accumulation for La, while PindSahibka (V-10) had the highest accumulation for Eu. The elemental accumulation analysis revealed a concentration at the centre of the Hoshiarpur district, where the sampling was conducted in various villages. From Fig. 6, it was estimated that among all samples, the accumulation was highest for La among the four rare earth elements; the calculated geo-accumulation index in soil was according to the trend: La > Sm > Yb > Eu. The marginal histogram graphically depict the distribution of elemental concentrations, dividing the data into equal intervals and representing the number of data points with horizontal bars. It reveals that the concentration of La was distributed over a range of approximately 8–13, with an outlier concentration of Sm falling within the range of

elemental Eu. It was also seen that a general accumulation index for the rare earth elements lies within 4–10 which shows significant elemental accumulation. The consistent application of roughly approximated doses of fertilizers to agricultural soil, which are the expected cause of the elevated levels of REEs (La, Sm, Yb and Eu), particularly those containing phosphate, and soil pH correctives such as lime, could also be contributing factors as hypothesized by Silva et al. (2019). Moreover examining the fertilizers and pesticides commonly utilized by farmers in the area will provide specific insights into the reasons behind REEs accumulation. According to previous studies there is a correlation between a higher atomic number and a decrease in the abundance of rare earth elements (REEs), observed in both even and odd sequences. The observation revealed that as the atomic number increased, the concentration of the element decreased in the earth’s crust. However, the mean concentration of Yb was determined to surpass that of both Eu and Sm. This trend underscored (in Fig. 7.) the environmental risk associated with this specific element (Yb) in the agricultural soil of

Table 7 Determined elemental concentrations (in mg kg⁻¹, otherwise indicated) for soil samples by EDXRF

Sample ID	Fe (mg/kg)	Ca (% by wt)	Mn (mg/kg)	Cr (mg/kg)	Rb (mg/kg)	Sr (mg/kg)	Pb (mg/kg)	Zr (mg/kg)	Zn (mg/kg)	Ti (mg/kg)
V-1	2.86±0.1	0.84±0.03	541.1±22	23.7±0.2	142±2.2	83.9±1	34±0.31	372.6±11.8	76.8±0.5	3665±54
V-2	2.85±0.1	0.83±0.03	638±22	BDL	129±2	62.4±0.8	29.6±0.27	91.8±2.9	58.9±0.4	2940±43
V-3	2.53±0.09	0.8±0.03	345.8±14	22.2±0.2	140±2.1	80.2±1	33.7±0.31	365.5±11.6	75.8±0.5	3153±46
V-4	2.73±0.1	0.74±0.03	799.2±16	BDL	133±2	69.7±0.9	30.2±0.28	98.8±3.1	60.5±0.4	3258±48
V-5	2.57±0.09	0.84±0.03	824.4±17	14.2±0.1	132±2	63.3±0.8	30.7±0.28	121.2±3.8	61±0.4	4402±65
V-6	2.73±0.1	0.83±0.03	825.7±18	13.4±0.1	120±1.8	32.4±0.4	29.6±0.27	40.3±1.3	60.1±0.4	4040±59
V-7	2.65±0.1	1.11±0.04	685.7±16	BDL	132±2	83.4±1	31.9±0.29	408.3±12.9	61.9±0.4	3709±54
V-8	2.45±0.09	0.48±0.02	694.9±29	7.8±0.1	143±2.2	95.4±1.2	29.4±0.27	84.3±2.7	70.5±0.5	4788±70
V-9	2.65±0.1	0.38±0.01	567.7±23	BDL	117±1.8	BDL	28.2±0.26	166.5±5.3	58±0.4	4774±70
V-10	3.81±0.14	0.66±0.02	1033.8±30	5.1±0	119±1.8	BDL	26.3±0.24	243.3±7.7	67.7±0.5	4649±68
V-11	3.46±0.13	0.65±0.02	716.5±29	BDL	149±2.3	20.2±0.2	32.2±0.29	203.9±6.4	77.7±0.5	3944±58
V-12	2.56±0.09	0.5±0.02	583.8±23	50.77±0.4	134±2	BDL	33.7±0.31	327±10.3	65.1±0.4	4038±59
V-13	2.61±0.1	0.43±0.02	816.2±17	BDL	139±2.1	10.9±0.1	29.9±0.27	235.5±7.4	65.8±0.4	3825±56
V-14	2.73±0.1	0.88±0.03	703±25	BDL	100±1.5	38.5±0.5	27.3±0.25	251±7.9	56.9±0.4	4220±62
V-15	3.09±0.11	0.87±0.03	990.1±16	BDL	126±1.9	BDL	28.9±0.26	384.5±12.2	57.9±0.4	3548±52
V-16	2.56±0.09	0.89±0.03	1162.8±19	32.9±0.2	124±1.9	BDL	28.8±0.26	116.2±3.7	95.5±0.6	3915±57
V-17	3.31±0.12	0.99±0.04	769.4±23	BDL	93±1.4	BDL	28.7±0.26	87.9±2.8	66.6±0.4	3494±51
V-18	2.62±0.1	0.87±0.03	1361.4±15	41.4±0.3	160±2.4	23.6±0.3	32.2±0.29	128.8±4.1	96.9±0.7	4690±69
V-19	2.76±0.1	0.88±0.03	836±18	12.8±0.1	151±2.3	BDL	29.1±0.27	262.4±8.3	81.4±0.5	3471±51
V-20	2.82±0.1	0.88±0.03	1040.5±18	24±0.2	152±2.3	157.2±1.9	30.8±0.28	149.2±4.7	85.7±0.6	3742±55
V-21	2.54±0.09	0.89±0.03	1001.5±21	25±0.2	115±1.8	BDL	25±0.23	250±7.9	62±0.4	3614±53
V-22	2.81±0.1	0.99±0.04	1140.5±19	20±0.1	145±2.2	45.6±0.6	34±0.31	311±9.8	55.6±0.4	4125±61

Table 8 Mean elemental concentrations (mg kg⁻¹/ % by wt as indicated) with global concentration for soil samples

Sr. No	Elements	Mean concentration	Standard dev	Global data
1	Si (%)	29.84 ± 0.78	3.22 ± 0.25	26–29
2	Na (%)	1.15 ± 0.18	0.15 ± 0.02	~2.8
3	Mg (%)	0.17 ± 0.06	0.06 ± 0.02	0.05–4
4	Al (%)	3.87 ± 0.04	1.37 ± 0.01	1–4
5	Ca (%)	0.77 ± 0.03	0.189 ± 0.008	~3.16
6	V (mg/kg)	37.02 ± 4.26	36.48 ± 4.20	10–500
7	Mn (mg/kg)	819 ± 66	236 ± 19	~437
8	K (%)	2.88 ± 0.11	0.58 ± 0.02	0.04–3
9	Co (mg/kg)	4.85 ± 0.03	7.45 ± 0.04	4.5–12
10	Ti (%)	3909 ± 390	523 ± 52	0.02–2.4
11	Sb (mg/kg)	0.51 ± 0.04	0.209 ± 0.022	0.05–4
12	Ba (mg/kg)	1576 ± 30	926 ± 11	550–668
13	Hf (mg/kg)	74.64 ± 3.70	52.33 ± 2.61	2–20
14	Ta (mg/kg)	0.49 ± 0.03	0.24 ± 0.09	0.2–5.3
15	Sc (mg/kg)	24.66 ± 46.82	7.45 ± 1.27	1.5–16.6
16	Fe (%)	28.048 ± 2804	3353 ± 335	0.1–10
17	Cr (mg/kg)	22.58 ± 2.25	13.04 ± 1.30	~54
18	Rb (mg/kg)	131.92 ± 13.19	16.74 ± 1.67	90–310
19	Sr (mg/kg)	39.26 ± 3.39	35.62 ± 3.57	260–730
20	Pb (mg/kg)	30 ± 3.02	2.4 ± 0.24	~25
21	Zr (mg/kg)	213.69 ± 21.36	112.68 ± 11.20	30–250
22	Zn (mg/kg)	69.04 ± 6.90	12.11 ± 1.22	10–300
23	Yb (mg/kg)	44.60 ± 2.56	37.78 ± 3.88	2.0–3.2
24	Sm (mg/kg)	34.35 ± 0.14	59.51 ± 0.22	3.5–7.1
25	La (mg/kg)	74.17 ± 0.88	98.44 ± 0.60	16–39
26	Eu (mg/kg)	3.13 ± 0.38	1.45 ± 0.17	1.1–2.0

Hoshiarpur, Punjab which highlights the accumulation issue of REEs.

Transition elements analysis

Manganese (Mn)

The quantification of elemental Mn was conducted using INAA-PCF and ED-XRF technique. Manganese compounds play a crucial role in soil composition as this element is vital for plant nutrition and influences the behavior of various other micronutrients. It is classified as an essential micronutrient for soil and plays a crucial role in stimulating root and plant growth. Upon data analysis, it became evident that most of the samples (except two) exceed the

permissible limit in soil (500 mg/kg), with the mean highest concentration observed in the Hoshiarpur region (1198 ± 51 mg/kg), while the mean lowest, falls within the permissible range at 400 ± 4 mg/kg. This finding underscores the significance of assessing manganese levels in soil, especially considering its impact on roots, plants, and potentially toxic elements. A plot shown in Fig. 8. described the elemental concentration of elemental Mn in all the collected samples in the study area.

Chromium (Cr)

Cr was quantified in arable soil samples, using the ED-XRF technique. It was observed that the mean values for Cr fell within the permissible limits recommended by WHO (150 mg/kg) (Ogundele et al., 2015). The chromium concentration in the samples

Table 9 REE I_{geo} index in study area soil for 22 samples

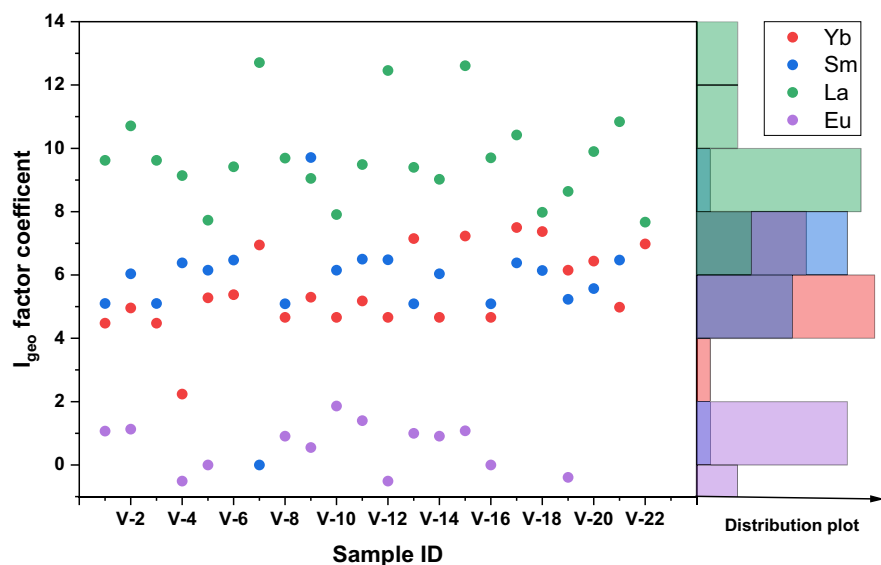
Sample ID	Yb	Sm	La	Eu
V-1	4.48	5.10	9.62	1.07
V-2	4.96	6.04	10.71	1.13
V-3	4.48	5.10	9.62	0.00
V-4	2.24	6.38	9.14	-0.51
V-5	5.28	6.15	7.73	0.00
V-6	5.38	6.47	9.42	0.00
V-7	6.95	0.00	12.71	0.00
V-8	4.66	5.09	9.69	0.91
V-9	5.30	9.71	9.05	0.55
V-10	4.66	6.15	7.91	1.86
V-11	5.18	6.50	9.49	1.40
V-12	4.66	6.48	12.46	-0.51
V-13	7.15	5.09	9.40	1.00
V-14	4.66	6.04	9.02	0.91
V-15	7.23	0.00	12.61	1.08
V-16	4.66	5.09	9.70	0.00
V-17	7.50	6.38	10.42	0.00
V-18	7.37	6.14	7.98	0.00
V-19	6.15	5.23	8.64	-0.39
V-20	6.44	5.57	9.90	0.00
V-21	4.98	6.47	10.84	0.00
V-22	6.98	0.00	7.67	0.00

ranged from 5.1 ± 0.5 mg/kg to 50 ± 5 mg/kg, with a mean concentration of 13.3 ± 2.2 mg/kg. Based on this data, it could be inferred that there was no significant potential harm posed by elemental chromium in the agricultural soils of the Punjab region. The highest chromium concentration was identified in Dasua (V-12) village of Hoshiarpur.

Zinc (Zn)

Zn, determined through the use of the ED-XRF technique, is considered an essential micronutrient crucial for soil health, playing a significant role in fostering root and plant growth. Upon thorough examination, it was apparent that all samples surpass the acceptable threshold (50 mg/kg) (Ogundele et al., 2015), in the study area registering the highest concentration of 96 ± 9 mg/kg (as shown in Fig. 9), while the lowest remains close to the permissible range, at 55 ± 5 mg/kg. It highlights the importance of evaluating soil zinc levels, mainly due to its influence on root and plant growth and its potential as a toxic element in agricultural soils. In this work, Zn exhibited an extended drainage period from soils, given its prolonged half-life as a soil pollutant. Managing Zn-contaminated soils often involves regulating its availability by applying lime or organic matter. The contamination of soils with Zn is a significant environmental concern. There is limited information available regarding the influence of zinc pollution. Typically, heavy

Fig. 6 Igeo scattering plot for study area soil samples with the horizontal elemental distribution



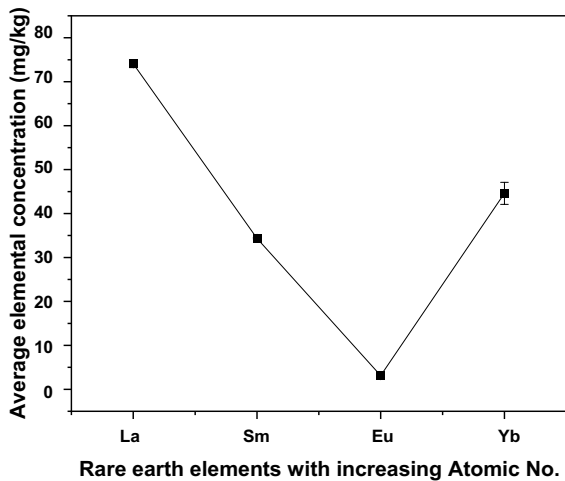
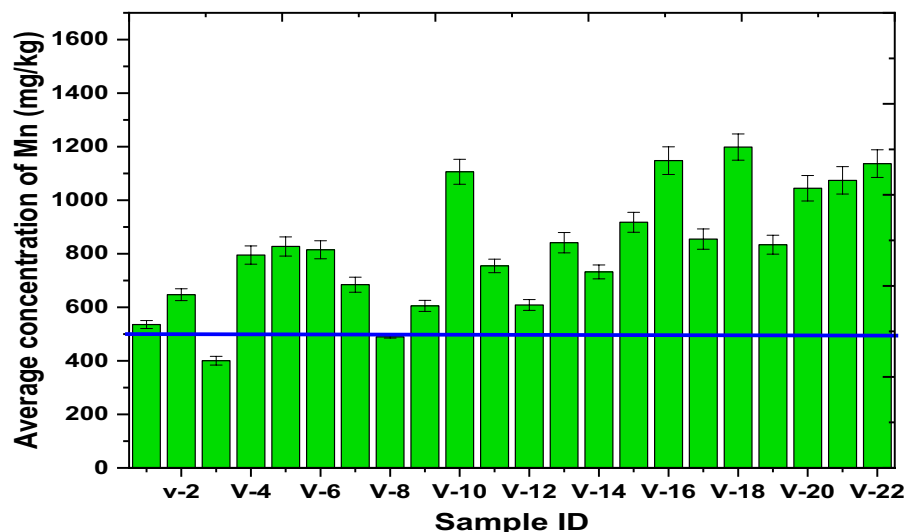


Fig. 7 Plot of average rare earth elements concentrations with the atomic number for the study site

metals exert a toxic effect on microbial communities when present in high concentrations in the soil. Studies have shown that elevated levels of metal contamination in soil can lead to a reduction in the diversity of microbial species, including both bacteria and fungi, particularly evident in bulk soils (Bolan et al., 8). The reason for such accumulation in study area soil was same cropping patterns followed by farmers such that there is no diversity and only partial elements get absorbed.

Fig. 8 Average elemental concentrations of Mn (mg/kg) in soil samples



Vanadium (V)

The measurement of vanadium levels in agricultural soil was conducted using the INAA-PCF technique. V is commonly found in the earth’s crust, ranking 22nd in abundance. Although elemental vanadium is not naturally occurring, it is present in approximately 65 different minerals, with patronite, roscoelite, carnotite, and vanadinite being the primary ore sources (Aide, 2005). The bar graph in Fig. 10 shows that the mean value of elemental vanadium in the study area was 37.04 ± 4.26 mg/kg. The highest value was measured in Birampur village (V4) of Hoshiarpur with V concentration of 170.29 ± 19.62 mg/kg, and the minimum value was 13.20 ± 1.52 mg/kg (V-14). According to (Wnuk, 2023), in Asia, the average optimum vanadium concentration in soil was in the range of 74–270 mg/kg. Notably, a specific set of samples exhibited a consistent rise in vanadium levels from sample V-4 to V-9 within the villages of Birampur (V-4), Bathehar (V-5), Bringli (V-6), Namoli (V-7), Sandhwal (V-8), and Patial (V-9) showing this trend. It was noteworthy that, apart from Birampur, all the villages were situated in the northern region, and Birampur, which displayed the highest concentration, was located in the southern part, so it may be estimated that these clusters of the samples had the same soil type and also approximately the same conditions or human activities. The average concentration of vanadium in the Earth’s crust, according to global data, is reported to be around 90 mg/kg. This suggests

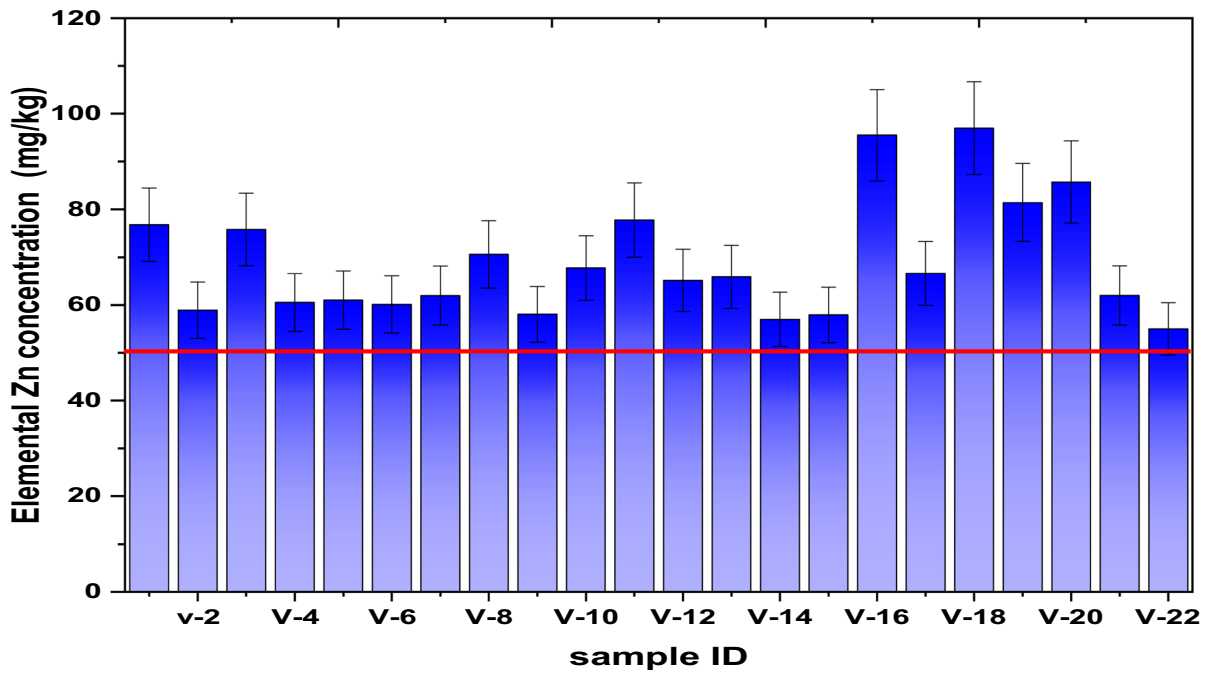


Fig. 9 Elemental concentrations of Zn (mg/kg) in soil samples

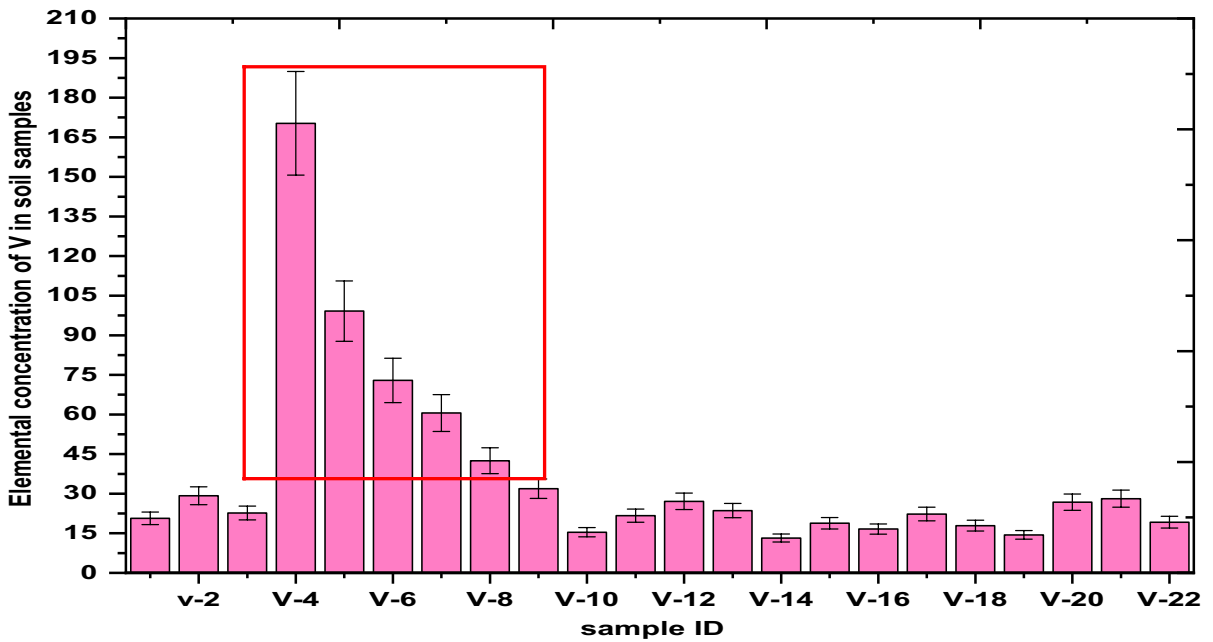


Fig. 10 Elemental concentrations of V (mg/kg) in soil samples

that the vanadium levels in our samples fall within the typical concentration observed globally. It's important to note that there isn't a universally established threshold for vanadium concentrations that signifies toxic behavior, as recognized by any organization. Hence, estimating the elemental concentration in crop yields may help to assess any potential impacts of elevated concentrations in the region with Birampur (V-4), Bathehar (V-5), Bringli (V-6), Namoli-Har (V-7), Sandhwal (V-8), and Patial (V-9) sites. As noted by Kabata et al., vanadium in soil is primarily associated with iron hydrous oxides and soil organic matter (SOM), with clay minerals also playing a role in its mobility. Topographically, the district can be classified into three main regions based on the soil-crop-climate complex as discussed earlier. We can infer that the concentration of V was higher in the Shivalik region and lower Shivalik beds compared to the flood plains. Therefore, besides fertilizer use, another contributing factor to the variation in elemental abundance could be the geological composition of mountainous terrain.

Titanium (Ti)

Titanium was assessed using the ED-XRF technique. Following a comprehensive investigation, it was found that the study area exhibited the highest titanium concentration, with levels reaching 4790 ± 70 mg/kg, while the lowest concentration was recorded at 2940 ± 43 mg/kg. This discovery highlights the importance of evaluating soil titanium levels, mainly due to its influence on root and plant growth and its potential as a toxic element. The mean Ti concentration was 3909 ± 57 mg/kg. As per the findings of Kabata-Pendias and Mukherjee (2007), the titanium content in surface soil globally falls within the range of 20–24000 mg/kg, with an average of 3300 mg/kg. All samples in our study fall within this established range...

Iron (Fe)

Iron is the fourth most abundant element on earth and an essential macro element. In collected soil samples, elemental iron was found within the 2.4–3.8% by weight (wt) range, with an average concentration of 2.8% by wt. Iron is considered an essential element for soil quality and human health, as it is a crucial

component in various proteins and enzymes and is essential for metabolism. Nevertheless, the iron content of soil is determined by a combination of parent rock composition and soil-related processes. Typically, the prevalent range of iron in soils generally falls between 0.5% by wt and 5% by wt; notably, all the samples studied were within this range. It was found that the highest concentration was found in the Pind-Sahibka village (V-10) and the minimum concentration was found in Sandhwal village (V-8). Kabata-Pendias and Mukherjee (2007) pointed out that manganese tends to accumulate in different soil horizons, especially those enriched in iron in the topsoil. However the correlation between Fe Vs Mn gives an $R^2=0.28$ which shows no significant correlation, It can further be analyzed that for the concentration of elemental Mn above ~ 1100 mg/kg there is correlation between concentration of Fe and Mn with the correlation coefficient of $R^2=0.81$.

Zirconium (Zr)

The elemental content of Zr was determined using the ED-XRF technique. The Zr content of soils is typically derived from parent rocks. Here the range of elemental concentration of Zr in the soil samples was from 40.3 ± 1.3 mg/kg to 408.3 ± 12.9 mg/kg, having the mean and standard deviation values of 213.6 ± 6.7 mg/kg and 112.6 ± 3.5 mg/kg. A high standard deviation indicates a wide spread of the concentration of Zr in the study area. The minimum and maximum values were found in Hoshiarpur's Bringli (V-6) and Namoli villages (V-7), respectively. According to Kabata-Pendias and Mukherjee (2007), the measured average Zr content across different soils was 224 mg/kg, so it was concluded that there was accumulation of elemental zirconium in the cultivated soil of Hoshiarpur.

Cobalt (Co)

Co levels were assessed using the INAA-SSF method. As per Kabata-Pendias and Mukherjee (2007) the permissible limit for elemental cobalt is set at 65 mg/kg. All cobalt measurements obtained from soil samples in our study were found to be below this threshold, indicating no environmental risk in the surface soil of the Hoshiarpur region. The average cobalt concentration was recorded at 4.85 ± 0.03 mg/kg. Lead (Pb):

The elemental content of Pb was determined using the ED-XRF technique. Two types of lead, primary and secondary, are recognized in terrestrial environments. Primary Pb originates geogenically and becomes incorporated into minerals during their formation, while secondary Pb has a radiogenic origin resulting from the decay of uranium (U) and thorium (Th). The geochemical properties of Pb^{2+} bear some resemblance to the divalent alkaline-earth group of metals. As a result, lead can substitute for K, Ba, Sr, and even Ca in both minerals and at sorption sites. The fate of anthropogenic Pb in soils has garnered significant interest lately due to its dual threat to humans and animals through the food chain and inhaling soil dust. The gradually mounting quantities of Pb in surface soils, including both arable and non-arable lands, have been reported in different terrestrial ecosystems (Kabata-Pendias and Mukherjee, 2007). Upon scrutinizing the soil samples, it was noted that the lead values for all the samples fell within the permissible limit (85 mg/kg) (Ogundele et al., 2015). Pb concentrations in the samples ranged from 25.1 ± 0.2 to 34.0 ± 0.3 mg/kg, with a mean concentration of 30.19 ± 0.27 mg/kg. This data suggested that elemental lead in the agricultural soils of the Punjab region did not pose a significant risk. The highest lead concentration was identified in the soil of Rattanpur village in Hoshiarpur.

We also measured Tantalum (Ta), Scandium (Sc) and Hafnium (Hf) utilizing INAA-SSF, in our research. Upon comparing our findings with global data, we noted significant differences. Hafnium levels ranged from 42 to 203 mg/kg, surpassing the global range of 2 to 20 mg/kg. Tantalum concentrations varied from 0.20 to 1.06 mg/kg, falling below the global average of 0.2 to 3.9 mg/kg. Scandium levels ranged from 47 to 202 mg/kg, contrasting with the global range of 1.5 to 16.6 mg/kg. These disparities highlight the importance of localized investigations. Understanding regional soil composition discrepancies is essential for agricultural practices. Other Macro and micro elemental analysis.

Aluminium (Al)

Elemental Al constitutes a significant portion of the Earth's crust, and in soil samples, its presence varies

within the range of 1.41–5.12% by wt with the average and standard deviation of about 3.58 ± 0.10 and $0.95 \pm 0.03\%$ by wt respectively. The sole stable and commonly encountered ion, Al^{3+} , is recognized for coordinating with oxygen ligands. This interaction with oxygen-bearing ligands highlights the versatile chemical nature of aluminium in soil environments. The highest and lowest values were found in Namoli and Sandhwal villages of Hoshiarpur, respectively.

Silicon (Si)

Si is the second most prevalent element in the Earth's crust, constituting an average of 28.8% by wt. While Si is not officially classified as an essential nutrient, numerous studies consistently showcase its positive impacts on plant growth and crop yields, underscoring its valuable contributions in agricultural contexts. In this work, the elemental concentration of Si was found within V-10, $23.30 \pm 0.59\%$ (Pind Sahibka) to V-16 $37.16 \pm 1.88\%$ (Adamwal). The average and standard deviation were found to be 29.84 ± 0.78 and $3.22 \pm 0.25\%$, respectively.

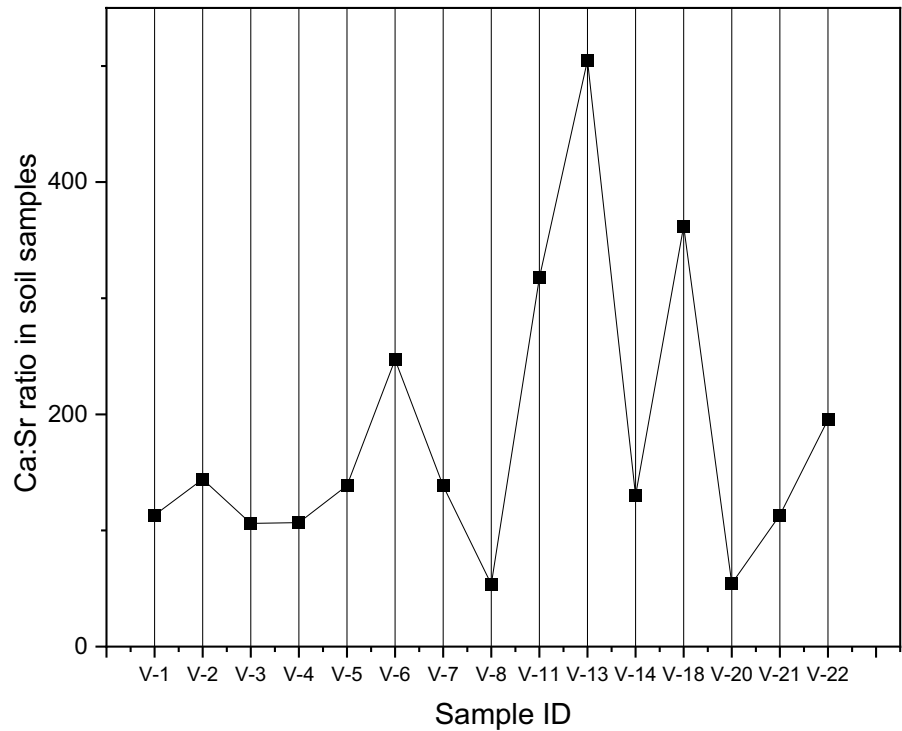
Magnesium (Mg)

The magnesium concentrations in the studied soil samples ranged from $0.080 \pm 0.002\%$ to $0.260 \pm 0.007\%$. Although no specific permissible values are established by organizations like UNEP, WHO and US-EPA, the general elemental magnesium concentration in all soil types typically falls between 0.05 and 4% by wt (Shreeja, 2021). This suggested that the manganese levels in the study area were within the natural range. Among the collected samples, Hoshiarpur (V-18) exhibited the highest concentration, while the lowest was observed in Kunail village (V-2) of Hoshiarpur district. The average concentration and standard deviation were 0.15 ± 0.003 and $0.05 \pm 0.001\%$ by wt, respectively.

Calcium (Ca)

Ca was estimated by both INAA- PCF and ED-XRF. Based on elemental analysis, the mean and standard deviation values for calcium concentrations in soil samples were reported as 0.77 ± 0.05 and $0.17 \pm 0.01\%$ by wt, respectively. The highest value was measured in Namoli- Har village (V-7),

Fig. 11 Describes the ratio of elemental Ca and Sr in soil samples (mg/kg)



and the lowest concentration was found in the Patial (V-9) village of Hoshiarpur, i.e. $1.13 \pm 0.09\%$ by wt $-0.40 \pm 0.02\%$ by wt. respectively while globally the mean concentration is approximately 3.16% wt.

This information is essential for understanding the variability of calcium levels in the soil and laid the groundwork for further investigation into potential patterns or influences on soil health and nutrient composition. Strontium is a frequently occurring trace element in the Earth’s crust, often linked with calcium (Ca) and, to a lesser extent, magnesium (Mg). The Sr to Ca ratio is typically consistent in the biosphere, serving as a common method for pinpointing elevated concentrations of Sr in a specific environment. However, our study reveals that the Sr to Ca ratio was not constant throughout all the samples, as indicated in Fig. 11. This instability could be attributed to other terrestrial activities influencing the arable land. Agricultural practices, including the use of fertilizers, pesticides, and irrigation methods, may introduce or redistribute strontium, affecting its concentration relative to calcium. Land use changes, such as urbanization, deforestation, or construction projects, can disturb natural soil compositions and introduce new sources of

strontium as well. Moreover, natural processes like weathering of rocks and minerals, volcanic eruptions, and erosion can influence the distribution of strontium in soil over time. Furthermore, improper disposal of industrial or municipal waste can result in contamination of soil with strontium, impacting its ratio with calcium. Investigating the influence of these terrestrial activities on soil composition and the Sr to Ca ratio can provide valuable insights into environmental factors affecting the study area and help in understanding the variability observed in the samples (Kabata-Pendia and Mukherjee, 2007).

Potassium (K)

Potassium’s elemental concentration was found between the range 2.4–5.1% by wt, while the average and standard deviation values were 2.8 ± 0.1 and $0.58 \pm 0.02\%$ by wt, respectively. The highest value of elemental K was found in Kunail (V-2) village of Hoshiarpur, and the lowest was measured in the Hoshiarpur region (V-18). It is considered to be the one of most essential element in agricultural soil. The concentration of elemental potassium in earth crust is 2.6% which reveals that in Hoshiarpur the value of

potassium is higher in agricultural soil due to application of fertilizers by farmers without prior knowledge of requirement of nutrients of soil and thus crop.

Rubidium (Rb) and Strontium (Sr)

The elemental concentrations of Rb and Sr ranged between 93 and 160 mg/kg and 11 to 95 mg/kg, respectively, with average and standard deviation values of 39 ± 3 and 131 ± 13 mg/kg and 16.1 ± 1.6 and 3.5 ± 0.3 mg/kg respectively. The Hoshiarpur region and Sandhwal of Hoshiarpur recorded the highest levels of elemental Rb and Sr, while the lowest concentrations were observed in Hazipur and Bhatiwala villages within Hoshiarpur, respectively.

Sodium (Na)

The average Na concentration is $1.50 \pm 0.03\%$ by wt. The minimum concentration was found in Bringli village ($1.02 \pm 0.02\%$ by wt) and the maximum in Namoli village ($2.54 \pm 0.05\%$ by wt).

Antimony (Sb) and Barium (Ba)

Our study in Punjab assessed Antimony (Sb) and Barium (Ba) concentrations in soil samples. Antimony levels ranged from 0.3 to 1.1 mg/kg, lower than the global average of 0.05 to 4.0 mg/kg. Conversely, Barium concentrations spanned 950 to 3855 mg/kg, significantly higher than the global range of 84 to 960 mg/kg.

Contamination assessment in soil (transition, heavy and toxic elements)

CF values for various elements were analyzed to assess their potential environmental impact. Among the elements examined, K and Co have CF values of 2.6 and 3.2, respectively, indicating considerable contamination. These elements pose a notable risk to environmental quality. Additionally, elements such as Na, Mg, Al, Mn, Ti, Sb, Ba, Hf, Ta, Sc, Fe, Rb, and Sr exhibit moderate contamination levels, and Si, Ca, V, Cr, Pb, Zr, and Zn demonstrate lower contamination in arable soil. Table 10 indicates the mean contamination factor in soil samples.

From the Potential Ecological Risk (PERI) factor, as given in Fig. 12 it can be seen that although from

Table 10 Average contamination factor calculated in soil samples collected from District Hoshiarpur

Sr. No	Elements	Contamination factor
1	Si	0.99
2	Na	1.05
3	Mg	1.21
4	Al	1.08
5	Ca	0.96
6	V	0.36
7	Mn	1.30
8	K	2.60
9	Co	3.20
10	Ti	1.14
11	Sb	1.06
12	Ba	1.57
13	Hf	1.08
14	Ta	1.01
15	Sc	1.09
16	Fe	1.07
17	Cr	0.90
18	Rb	1.34
19	Sr	1.18
20	Pb	0.91
21	Zr	1.04
22	Zn	1.10

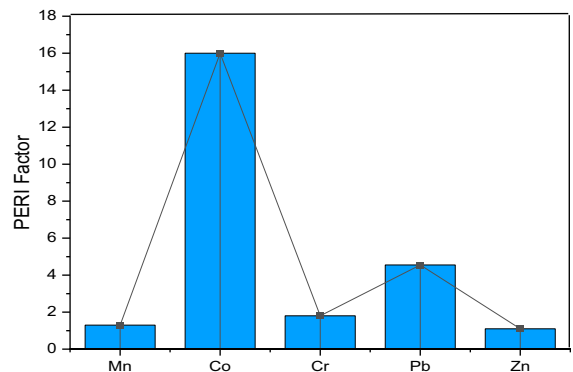


Fig. 12 Appraisal of potential ecological risk

the uncultivated land, the concentrations of Co and Pb are high, which may cause severe contamination. Moreover the risk of elemental pollution risk was $Co > Pb > Cr > Mn > Zn$.

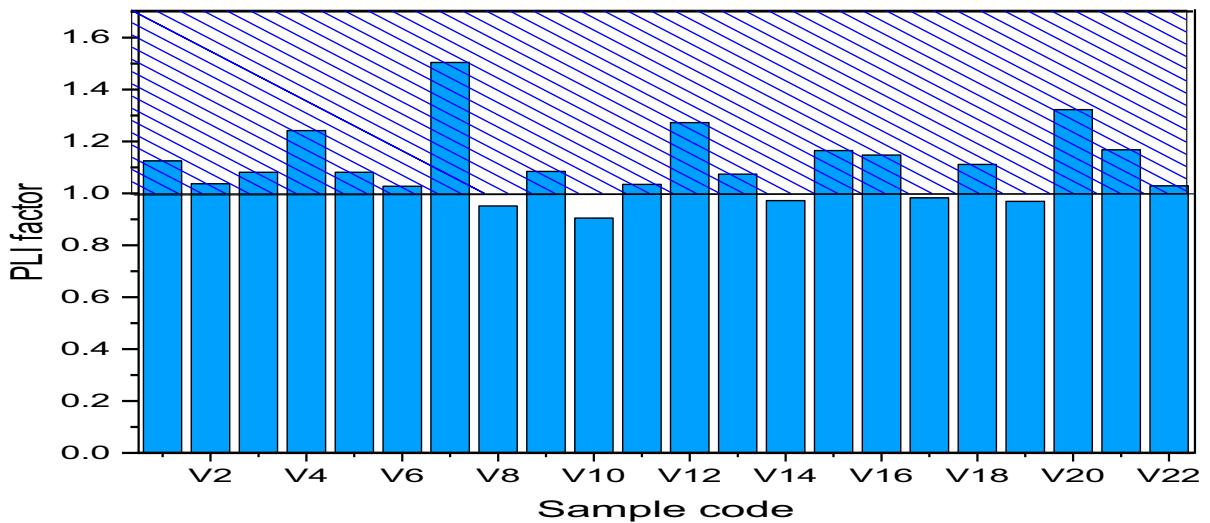


Fig. 13 PLI of the soil samples investigated

In the environmental quality investigation, we employed the Pollution Load Index (PLI) to gauge the pollution status of a given dataset. The PLI values were categorized into distinct ranges: $PLI \leq 1$ denoting an unpolluted state, 1–3 indicating moderate pollution, 3–5 representing high pollution, and values ≥ 5 signifying very high pollution levels. The subsequent analysis of the dataset shown in Fig. 13, accompanied by the respective sample codes, revealed the following insights: V8, V10, V14, V17 and V19 exhibited PLI values less than 1, characterizing them as unpolluted. Conversely, V1, V2 V3, V4, V5, V6, V7, V9, V11, V12, V13, V14, V15, V16, V18, V20, V21, and V22 displayed PLI values ranging from 1 to 1.5, categorizing them as moderately polluted. The Bar graph in Fig. 13 shows the PLI factor for collected agricultural samples. Site 7 appears to be the most polluted, followed by sites V-20 and V4 and V12. Understanding the specific sources and pathways of pollution at these agricultural sites requires further detailed environmental assessments and monitoring to mitigate potential risks to human health and the environment. Possible reasons for the higher pollution levels observed at agricultural sites could include various factors such as the use of chemical fertilizers may lead to soil and water contamination if applied improperly or excessively. Historical contamination from previous land use practices and natural sources like geological formations may also play a role in

contributing to elevated pollution levels. Inadequate waste management practices, such as inadequate sewage treatment or landfill management, may further exacerbate pollution in agricultural areas.

Conclusion

In this study, soil samples were subjected to analysis using three distinct methods: INAA- PCF and SSF, IBA-PIGE, and ED-XRF. Notably, the ED-XRF technique, a widely adopted X-ray-based method, facilitated rapid assessment of major and minor elemental compositions. This preliminary data proved invaluable for subsequent quantitative analyses using other techniques such as IBA and INAA. Method validation was ensured through the examination of certified reference materials (USGS CRM AGV-1 and RGM-1) which demonstrated good agreement with certified values. The analysis of 22 agricultural soil samples encompassed 26 elements, focusing particularly on minor, major and trace level elements, thereby revealing their significant presence and elucidating potential environmental risks within the Hoshiarpur district of Punjab. The study focused on investigating the distribution and accumulation of REEs using the INAA-SSF method, revealing notable contamination for elements such as La, Sm, and Yb. Spatial analysis identified regions with elevated concentrations, with

Hazipur and Hoshiarpur showing high accumulation of Yb, while Patial and Namoli-Har exhibited heightened concentrations of Sm and La, respectively. Concurrently, the assessment of six essential elements—K, Mn, Zn, Fe, Ca, and Mg—underscored the risk of accumulation in arable soil for Mn and Zn when compared with permissible limits. Notably, 90% of soil samples had higher concentrations of Mn, while all samples exceeded permissible levels for Zn, posing a significant environmental concern. The study also found elevated concentrations of elemental K compared to global soil levels, suggesting excessive use of potassium-based fertilizers in Hoshiarpur agricultural soil. Furthermore, varying vanadium concentrations were observed across different regions of the Hoshiarpur district, with the highest values recorded in Birampur village (V-4), followed by Bringli (V-6), Namoli (V-7), Sandhwal (V-8), and Patial (V-9). These findings highlight the combined influence of geological factors and human activities on elemental abundance in agricultural soil. In addition, ecological risk factors were calculated for other quantified elements, revealing a trend where K exhibited the highest concentration. The study emphasized the improper use of potassium-based fertilizers by farmers, contributing to soil accumulation. To analyze other quantified elements, ecological risk factors were calculated in which we calculate different factors like CF, PERI and PLI. We found the observed trend for the studied elements as: $K > Co > Ba > Mn = Hf = Rb = Sc > Mg = Ta = Sr = Sb > Na = Al = Ti = Fe = Zn > Ca = Si = Zr > Pb > Cr > V$. Overall, the findings suggest that elemental accumulation can potentially bio-accumulate in crops, emphasizing the need for advanced agricultural technologies to prevent contaminant discharge and mitigate environmental risks in the Hoshiarpur district. This underscores the significance of soil quality and pollution analysis in addressing environmental concerns in the region. Further research is needed to explore the long-term implications of elemental accumulation. It's crucial to look into what happens over a long time period when elements build up in crops. This will also help to understand how it affects farming in the long run and the environment in Hoshiarpur region of Punjab.

Acknowledgements Authors from SGTB Khalsa College, Sri Anandpur Sahib-Punjab want to acknowledge UGC-DAE-CSR (Project Sanction No. CRS/2021-22/03/567) to allow the

Project Fellow to carry out R&D work at RCD, BARC, Mumbai with Dr R Acharya as Principal Collaborator. The authors extend their sincere appreciation to Dr. P. K. Mohapatra, Associate Director of Radiochemistry and Isotope Group, and Head of Radiochemistry Division, for granting necessary permissions and providing valuable guidance.

Author contributions DS and RA contributed to the study's conception and design and monitored the work's progress. VD and SG did material preparation and data collection. DS and VM analyzed the results. DS and VD wrote the first draft of the manuscript. All the authors commented on the final versions of the manuscript. All the authors read and approved the final manuscript. Additionally, each author affirms that the material presented in the manuscript has not been previously submitted to or published in any other publication before its submission to the Environmental Geochemistry and Health.

Funding All the authors gratefully acknowledge the funding received under the UGC-DAE-CSR project (Sanction No. CRS/2021-22/03/567).

Data availability The data used to support the findings of this study are included in the article.

Declarations

Conflict of interest All co-authors have seen and agree with the manuscript's contents and have complied as applicable with the statement on "Ethical responsibility of Authors". The authors have no potential conflicts of interest to declare. The authors declare that they have no known competing financial interests or personal relationships that could have appeared to influence the work reported in this paper.

References

- Abrahams, P. W. (2002). Soils: Their implications to human health. *Science of the Total Environment*, 291(1–3), 1–32. [https://doi.org/10.1016/S0048-9697\(01\)01102-0](https://doi.org/10.1016/S0048-9697(01)01102-0)
- Acharya, R., & Pujari, P. K. (2019). Potential of conventional and internal monostandard NAA and PGNA and PIGE in forensic sciences: An overview. *Forensic Chemistry*, 12, 107–116. <https://doi.org/10.1016/j.forc.2018.01.002>
- Aide, M. (2005). Geochemical assessment of iron and vanadium relationships in oxic soil environments. *Soil & Sediment Contamination*, 14(5), 403–416. <https://doi.org/10.1080/15320380500180382>
- Alexandratos, N. & Bruinsma, J. (2012). World agriculture towards 2030/2050: The 2012 revision.
- Amonette, J. E., & Sanders, R. W. (1994). Nondestructive techniques for bulk elemental analysis. *Quantitative methods in soil mineralogy* (pp. 1–48). Amsterdam: Elsevier.
- Bacon, J. R., Butler, O. T., Cairns, W. R., Cavoura, O., Cook, J. M., Davidson, C. M., & Mertz-Kraus, R. (2023). Atomic spectrometry update—a review of advances in environmental analysis. *Journal of Analytical Atomic Spectrometry*. <https://doi.org/10.1039/D3JA90013D>

- Balaram, V. (2021). Current and emerging analytical techniques for geochemical and geochronological studies. *Geological Journal*, 56(5), 2300–2359. <https://doi.org/10.1002/gj.4005>
- Bolan, N., Kunhikrishnan, A., Thangarajan, R., Kumpiene, J., Park, J., Makino, T., & Scheckel, K. (2014). Remediation of heavy metal (loid)s contaminated soils—to mobilize or to immobilize? *Journal of Hazardous Materials*, 266, 141–166. <https://doi.org/10.1016/j.jhazmat.2013.12.018>
- Chambhare, N. M., Ghaywat, S. D., & Lohiya, J. (2021). Recent basic advances of neutron activation analysis. *Journal of Global Trends in Pharmaceutical Sciences*, 12(4), 9873–9887.
- Custo, G., Boeykens, S., Dawidowski, L., Fox, L., Ómez, D. G., Una, F. L., & Vázquez, C. (2005). Soil characterization by energy dispersive X-ray fluorescence: Sampling strategy for in situ analysis. *Analytical Sciences*, 21(7), 751–756. <https://doi.org/10.2116/analsci.21.751>
- Dey, A., Dasgupta, S., Sengupta, S., Dutta, S., Mukhopadhyay, S., & Majumder, S. P. (2023). Food security and carbon footprint: Lessons from COVID-19 in the Indian subcontinent. *Handbook of energy management in agriculture* (pp. 1–25). Singapore: Springer Nature Singapore.
- Dhorge, P. S., Acharya, R., Rajurkar, N. S., Chahar, V., Tuli, V., Srivastava, A., & Pujari, P. K. (2017). Quantification of trace fluorine concentrations in soil and food samples from fluoride affected region by in situ current normalized particle induced gamma-ray emission method. *Journal of Radioanalytical and Nuclear Chemistry*, 311, 1803–1809. <https://doi.org/10.1007/s10967-016-5118-5>
- El-Taher, A. (2018). Nuclear analytical techniques for detection of rare earth elements. *Journal of Radiation and Nuclear Applications*, 3(1), 53–64. <https://doi.org/10.18576/jrna/030107>
- Esen, A. N., Azbouche, A., Hacıyakupoğlu, S., Erentürk, S., & Melzi, Z. (2024). Accumulation of heavy metals and determination of natural radioactivity in the soil-thyme system in Omerli, Istanbul: Assessment of ecological and health risk. *Gazi University Journal of Science*, 37, 1–1.
- Gruhn, P., Goletti, F., & Yudelman, M. (2000). Integrated nutrient management, soil fertility, and sustainable agriculture: current issues and future challenges. *International Food Policy Research Institute*, 6, 4.
- Gupta, S. B., BabyKumar, A., & Singh, V. (2023). Selenium uptake and immobilization using indigenous *Bacillus* strain isolated from seleniferous soils of Punjab. *Bioremediation Journal*, 27(4), 434–442. <https://doi.org/10.1080/10889868.2022.2040414>
- Haruna, A., & Yahaya, S. M. (2021). Recent advances in the chemistry of bioactive compounds from plants and soil microbes: A review. *Chemistry Africa*, 4(2), 231–248. <https://doi.org/10.1007/s42250-020-00213-9>
- Kabata-Pendias, A., & Mukherjee, A. B. (2007). *Trace elements from soils to human*. Berlin, Heidelberg: Springer-Verlag.
- Kesavan, P. C., & Swaminathan, M. (2008). Strategies and models for agricultural sustainability in developing Asian countries. *Philosophical Transactions of the Royal Society B: Biological Sciences*, 363(1492), 877–891. <https://doi.org/10.1098/rstb.2007.2189>
- Kim, H., Hwang, H., & Ro, C. U. (2006). Single-particle characterization of soil samples collected at various arid areas of China, using low-Z particle electron probe X-ray microanalysis. *SpectrochimicaActa Part B: Atomic Spectroscopy*, 61(4), 393–399. <https://doi.org/10.1016/j.sab.2006.01.012>
- Lee, Y. L., Chang, C. C., & Jiang, S. J. (2003). Laser ablation inductively coupled plasma mass spectrometry for the determination of trace elements in soil. *SpectrochimicaActa Part B: Atomic Spectroscopy*, 58(3), 523–530. [https://doi.org/10.1016/S0584-8547\(03\)00007-7](https://doi.org/10.1016/S0584-8547(03)00007-7)
- Lehmann, J., Bossio, D. A., Kögel-Knabner, I., & Rillig, M. C. (2020). The concept and future prospects of soil health. *Nature Reviews Earth & Environment*, 1(10), 544–553. <https://doi.org/10.1038/s43017-020-0080-8>
- Maenhaut, W. (1992). Trace element analysis of environmental samples by nuclear analytical techniques. *International Journal of PIXE*, 2(04), 609–635. <https://doi.org/10.1142/S0129083592000658>
- Melaku, S., Dams, R., & Moens, L. (2005). Determination of trace elements in agricultural soil samples by inductively coupled plasma-mass spectrometry: microwave acid digestion versus aqua regia extraction. *AnalyticaChimicaActa*, 543(1–2), 117–123. <https://doi.org/10.1016/j.aca.2005.04.055>
- Muller, G. (1969). Index of geoaccumulation in sediments of the Rhine River. *GeoJournal*, 2, 108–118.
- Ogundele, D. T., Adio, A. A., & Oludele, O. E. (2015). Heavy metal concentrations in plants and soil along heavy traffic roads in North Central Nigeria. *Journal of Environmental & Analytical Toxicology*, 5(6), 1. <https://doi.org/10.4172/2161-0525.1000334>
- Peng, S., Peng, T., & Sun, G. (2022). Progress on nuclear analysis techniques. *Nuclear Analysis*, 1(1), 100007. <https://doi.org/10.1016/j.nucana.2022.100007>
- Pimentel, D., Berger, B., Filiberto, D., Newton, M., Wolfe, B., Karabinakis, E., & Nandagopal, S. (2004). Water resources: Agricultural and environmental issues. *BioScience*, 54(10), 909–918.
- Raja, S. W., & Acharya, R. (2023). Development of an external PIGE method using nitrogen from atmospheric air as external beam current normalizer and its application to nondestructive quantification of total boron mass fraction in boron containing neutron absorbers. *AnalyticaChimicaActa*, 1266, 341353. <https://doi.org/10.1016/j.aca.2023.341353>
- Rosegrant, M. W., Ringler, C., & Zhu, T. (2009). Water for agriculture: Maintaining food security under growing scarcity. *Annual Review of Environment and Resources*, 34, 205–222.
- Samanta, S. K., Raja, S. W., Sharma, V., Girkar, P. S., Acharya, R., & Pujari, P. K. (2020). Development of an external (in air) in situ current normalized particle induced gamma-ray emission method utilizing 3.5 MeV proton beam from FOTIA for rapid quantification of low Z elements in glass and ceramic samples. *Journal of Radioanalytical and Nuclear Chemistry*, 325, 923–931. <https://doi.org/10.1007/s10967-020-07266-7>
- Sharma, N., Prakash, R., Srivastava, A., Sadana, U. S., Acharya, R., Prakash, N. T., & Reddy, A. R. (2009). Profile of selenium in soil and crops in seleniferous area of Punjab,

- India by neutron activation analysis. *Journal of Radio-analytical and Nuclear Chemistry*, 281, 59–62. <https://doi.org/10.1007/s10967-009-0082-y>
- Sharma, V., Acharya, R., Bagla, H. K., & Pujari, P. K. (2021). Standardization of an external (in air) PIGE methodology using tantalum as a current normalizer in conjunction with INAA for rapid and non-destructive chemical characterization of “as-received” glass fragments towards forensic applications. *Journal of Analytical Atomic Spectrometry*, 36(3), 630–643. <https://doi.org/10.1039/D0JA00482K>
- Sharma, V., Sarkar, A., Acharya, R., Bagla, H. K., & Pujari, P. K. (2022). Utilization of accelerator and reactor based nuclear analytical techniques for chemical characterization of automobile windshield glass samples and potential of statistical analyses using trace elements towards glass forensics. *Forensic Science International*, 334, 111262. <https://doi.org/10.1016/j.forsciint.2022.111262>
- Shikha, D., Dadwal, V., Kapil, C., Singha, G., Mehta, V., & Acharya, R. (2023). Assessment of macronutrients and physicochemical parameters of agricultural soils in Nawanshahr-Hoshiarpur districts of Punjab. *Indian Journal of Pure & Applied Physics*. <https://doi.org/10.56042/ijpap.v61i6.2408>
- Shreeja, D. (2021). Magnesium: Forms, sources and behavior soil (soilmanagementindia.com) Accessed on December 12
- Silva, F. B. V., Nascimento, C. W. A., Alvarez, A. M., & Araújo, P. R. M. (2019). Inputs of rare earth elements in Brazilian agricultural soils via P-containing fertilizers and soil correctives. *Journal of Environmental Management*, 232, 90–96. <https://doi.org/10.1016/j.jenvman.2018.11.031>
- Solangi, F., Zhu, X., Khan, S., Rais, N., Majeed, A., Sabir, M. A., & Kayabasi, E. T. (2023). The global dilemma of soil legacy phosphorus and its improvement strategies under recent changes in agro-ecosystem sustainability. *ACS Omega*, 8(26), 23271–23282. <https://doi.org/10.1021/acsomega.3c00823>
- Srivastava, A., Bains, G. S., Acharya, R., & Reddy, A. V. R. (2011). Study of seleniferous soils using instrumental neutron activation analysis. *Applied Radiation and Isotopes*, 69(5), 818–821. <https://doi.org/10.1016/j.apradiso.2011.01.027>
- Swaminathan, M. S. (2017). *50 years of green revolution: An anthology of research papers* (Vol. 1). Singapore: World Scientific Publishing Company.
- Taiwo, A. M., Michael, J. O., Gbadebo, A. M., et al. (2019). Pollution and health risk assessment of road dust from Osogbo metropolis, Osun state, Southwestern Nigeria. *Human and Ecological Risk Assessment*. <https://doi.org/10.1080/10807039.2018.1563478>
- Vasu, D., Tiwary, P., Chandran, P., & Singh, S. K. (2020). Soil quality for sustainable agriculture. *Nutrient Dynamics for Sustainable Crop Production*. https://doi.org/10.1007/978-981-13-8660-2_2
- Verma, H. R. (2007). *Atomic and nuclear analytical methods*. Berlin Heidelberg: Springer-Verlag.
- Wnuk, E. (2023). Mobility, bioavailability, and toxicity of vanadium regulated by physicochemical and biological properties of the soil. *Journal Soil Science Plant Nutrients*, 23, 1386–1396. <https://doi.org/10.1007/s42729-023-01130-9>
- Yang, S. Y., Jiang, S. Y., Mao, Q., Chen, Z. Y., Rao, C., & Li, X. (2022). Electron probe microanalysis in geosciences: Analytical procedures and recent advances. *Atom Spectroscopy*, 43, 186–200. <https://doi.org/10.46770/AS.2021.1013>

Publisher's Note Springer Nature remains neutral with regard to jurisdictional claims in published maps and institutional affiliations.

Springer Nature or its licensor (e.g. a society or other partner) holds exclusive rights to this article under a publishing agreement with the author(s) or other rightsholder(s); author self-archiving of the accepted manuscript version of this article is solely governed by the terms of such publishing agreement and applicable law.